



Carlos Miguel Branquinho Ferreira de Jesus Monteiro

Bachelor of Science

Cellular proliferation in 3D Tissue Engineering scaffolds made of polymeric nano-fibers

Dissertation submitted in partial fulfillment
of the requirements for the degree of

Master of Science in
Biomedical Engineering

Adviser: Jorge Carvalho Silva, Assistant Professor,
NOVA University of Lisbon

Co-adviser: Célia Reis Henriques, Assistant
Professor, NOVA University of Lisbon

Examination Committee

Chair: Carla Quintão Pereira, Assistant Professor, NOVA University of Lisbon
Rapporteurs: Susana Filipe Barreiros, Associate Professor, NOVA University of Lisbon
Jorge Carvalho Silva, Assistant Professor, NOVA University of Lisbon



FACULDADE DE
CIÊNCIAS E TECNOLOGIA
UNIVERSIDADE NOVA DE LISBOA

June, 2019

Cellular proliferation in 3D Tissue Engineering scaffolds made of polymeric nano-fibers

Copyright © Carlos Miguel Branquinho Ferreira de Jesus Monteiro, Faculty of Sciences and Technology, NOVA University Lisbon.

The Faculty of Sciences and Technology and the NOVA University Lisbon have the right, perpetual and without geographical boundaries, to file and publish this dissertation through printed copies reproduced on paper or on digital form, or by any other means known or that may be invented, and to disseminate through scientific repositories and admit its copying and distribution for non-commercial, educational or research purposes, as long as credit is given to the author and editor.

ACKNOWLEDGEMENTS

In the closing of this incredible cycle, full of challenges that made me grow academically and as a person, there are many people to whom I owe my thanks.

I would like to acknowledge the institution NOVA University of Lisbon and in particular the Faculty of Science and Technology, which has proved to be an organization that presents his students a truly challenging, rigorous but equally rewarding educational program.

I want to thank all the Professors who have been part of my student journey, from kindergarten to masters. Everyone was important in their own way and everyone taught me something valuable for life.

I want to thank my advisor, Professor Jorge Carvalho Silva, who taught me a lot about Tissue Engineering and was always ready to help throughout my dissertation, always with the greatest commitment, comprehension, and appreciation for teaching.

My co-advisor, Professor Célia Henriques, who besides my mentor was also my Teacher of Vibrations and Waves, I want to thank not only for being always available to support but also for having given me some of the best-prepared classes I have ever attended.

I would like to thank the people of the Department of Materials Science and CENIMAT/I3N for their collaboration in this project.

Thanks to my GREAT lab colleagues, Diana Querido, and José Vilhena.

A special thanks to my colleagues and friends, particularly those who labored alongside me in this final cycle, Pedro Silva and João Lopes.

A big thank you and hug to my great buddy Ricardo Mateus, whom with his friendship and laughs made this path much more bearable - You are a friend for life.

I want to thank Karina Freitas, the great love of my life. I'm very lucky to have grown up with you and to have learned so much from you. Your love and support were fundamental in this journey and without it, I couldn't have done it. You make me a better and stronger man.

I want to thank my grandmother Cacilda, I know that one of your dreams was to see me graduated from University, you may be old and not remember me well, but I'll never forget you. Thank you for educating me and for all the patience you had for me.

I want to thank my parents, who made me what I am today, for all the moments and dedication they had to me. For all the affection, love and education they gave me. They are the best parents in the world and I hope I can return all this love.

*"The leading project of the Scientific Revolution is to give
humankind eternal life." - Yuval Noah Harari*

ABSTRACT

The extracellular matrix, a component of all animal tissues, is required for cell adhesion, migration and proliferation to provide support to the regulation of cellular activity. The extracellular matrix acts as a reservoir of hormones, growth factors, and intercellular communication medium. In Tissue Engineering, a number of techniques are utilized, namely the electrospinning of polymeric nanofibers, for the production of biodegradable porous 3D scaffolds that attempt to mimic the native extracellular matrix structure.

This work proposes to investigate the impact that the combination of the application of poly(ethylene oxide) sacrificial fibers with sucrose as a porogenic agent has on the ability of cellular infiltration inside a porous 3D matrix made of polycaprolactone and gelatine.

The characterization of the structural and physicochemical properties of the fabricated scaffolds was made. Structural characterization was performed by means of optical and electronic microscopy. In order to understand the physicochemical characteristics, mechanical tensile tests, mass loss, infrared spectroscopy and fluorescence assays were conducted.

The interpretation of these results revealed fibers with morphology comparable to the native extracellular matrix, scaffolds with good mechanical properties and good reproducibility. In vitro assays revealed that the models provide good cell adhesion and proliferation.

Keywords: Polycaprolactone; Gelatine; Polyethylene oxide; Sacrificial Fibers; Porogenic Agent; Electrospinning.

RESUMO

A matriz extracelular constituinte de todos os tecidos animais é necessária para a adesão, migração e proliferação celular, além de dar apoio à regulação da atividade celular por ser um reservatório de hormonas, fatores de crescimento e meio de comunicação intercelular. Na Engenharia de Tecidos são usadas diversas técnicas, nomeadamente a eletrofição de nano-fibras poliméricas, para a produção de matrizes 3D porosas biodegradáveis que tentam mimetizar a estrutura da matriz extracelular nativa.

Este trabalho teve como objetivo estudar o impacto que a combinação da utilização de poli(óxido de etileno) como fibras sacrificiais com um agente porogénico têm na capacidade de infiltração celular no interior de uma matriz 3D porosa composta por policaprolactona e gelatina.

Foi feita a caracterização das propriedades estruturais e físico-químicas das matrizes fabricadas. Para a caracterização estrutural foram utilizadas técnicas de análise por microscopia ótica e electrónica de varrimento. Para compreender as propriedades físico-químicas, foram feitos ensaios mecânicos de tração, perda de massa, espectroscopia de infravermelho e fluorescência.

A análise destes resultados demonstrou fibras com morfologia semelhante à matriz extracelular nativa, matrizes com boas propriedades mecânicas e boa reprodutibilidade de produção. Os ensaios *in vitro* revelaram que as matrizes proporcionam uma boa adesão e proliferação celular.

Palavras-chave: Policaprolactona; Gelatina; Polióxido de etileno; Fibras Sacrificiais; Agente Porogénico; Electrofição.

CONTENTS

1	Introduction	1
1.1	Contextualization	1
1.2	Framework	2
1.2.1	Extra Cellular Matrix	2
1.2.2	Pore Size and Porosity	2
1.2.3	3D Scaffolds Production Techniques	3
1.2.4	Leaching of a Porogenic Agent	3
1.2.5	Use of Sacrificial Fibers	4
1.2.6	Electrospinning	4
1.3	State of Art	5
1.3.1	Reference of the Use of Porogenic Agents	6
1.3.1.1	Sucrose as a Porogenic Agent	7
1.3.2	Reference to the Use of Sacrificial Fibers	8
1.3.3	Reference to the Combination of a Porogenic Agent with Sacrificial Fibers	9
2	Materials and Methods	11
2.1	Materials	11
2.1.1	Polycaprolactone	11
2.1.2	Gelatin	12
2.1.3	Combination of PCL with Gelatin	12
2.1.4	Polyethylene Oxide	12
2.2	Solutions	12
2.2.1	Preparation of Solutions	13
2.2.1.1	Production of Sucrose Crystals in Different Granulometry	15
2.2.1.2	Procedures for the Production of Solutions	15
2.3	Scaffold Production	16
2.3.1	Experimental Arrangement	16
2.3.2	Eletrospinning Parameters	17
2.3.3	Scaffold Crosslinking	19
2.3.4	Scaffold Washing	20
2.4	Scaffold Characterization	20

CONTENTS

2.4.1	Morphological Analysis	20
2.4.2	ATR-FTIR	21
2.4.3	Mass Loss Assays	22
2.4.4	Fluorescence Assays	23
2.4.5	Tensile Tests	24
2.5	<i>In Vitro</i> Assays	26
2.5.1	Preparation of Samples for Cell Culture	26
2.5.2	Cell Culture with the HFFF2 Cell Line	27
2.5.3	Cell Culture Viability Assays	28
2.5.4	Cell Culture Infiltration Assays	28
3	Presentation and Discussion of Results	31
3.1	Determination of the Scaffolds Production Parameters	31
3.2	Scaffolds Characterization	43
3.2.1	Morphology	43
3.2.1.1	After Electrospinning	43
3.2.1.2	After Crosslinking	45
3.2.1.3	After Washing	46
3.2.2	Mass Loss Assays	49
3.2.3	ATR-FTIR	50
3.2.4	Fluorescence Assays	53
3.2.5	Tensile Tests	55
3.3	<i>In Vitro</i> Assays	57
3.3.1	Adhesion and Proliferation	57
3.3.2	Cell Infiltration	57
4	Conclusions and Future Perspectives	61
	Bibliography	65

LIST OF FIGURES

1.1	A typical arrangement of the electro-spinning technique. In this particular case, with a vertical axis arrangement of the electrodes [11].	5
1.2	Electrospinning of a polymer and formation of the Taylor cone due to the accumulation of charges to the surface of the solution in the presence of an electric field.	6
1.3	Technique for the use of porogenic agents. (A) Schematic, with the electro-spinning process and the porogen being sifted over the electrospun scaffold. (B) Photograph of the resulting porous matrix [18].	6
1.4	SEM images of: (A) non-porous PCL fibers; (B) surface morphology of a porous PCL matrix; (C) matrix before salt leaching; (D) matrix after saltleaching. [36]	7
1.5	Density, porosity and pore size of PLGA matrices prepared using two different porogen agents (NaCl or Sucrose) [8].	8
2.1	Solutions aspect.	14
2.2	Equipment utilized to mill and grade the sucrose crystals.	15
2.3	Experimental Arrangement.	16
2.4	Post-electrospun scaffold inside the desiccator.	18
2.5	Scaffold fixed to a flat metal plate.	19
2.6	Crosslinking container with two crystallizers inside.	20
2.7	Metallic discs with scaffold samples ready to be analyzed on SEM.	21
2.8	ATR-FTIR equipment.	22
2.9	PCL and PEO solutions doped with Rhodamine B and Fluorescein respectively.	24
2.10	Sample being tractioned.	25
2.11	Teflon supports mounted on a 24-well plate.	27
2.12	Schematic representation of the reduction of resazurin to resorufin by the enzyme NAD (nicotinamide adenine and dinucleotide) by metabolically active cells. [adapted from http://file.biotoool.com/downloads/Vita-Blue-Cell-Viability-Reagent.pdf]	28
2.13	The 96 well plate ready to be analyzed.	29
2.14	The 96 well plate mounted on the UV absorbance plate reader.	29
2.15	Nuclear labeling of cells with DAPI at GREAT cell culture laboratory.	29
3.1	The formation of beads along the fibers.	32

3.2	Fibers with good morphology but with beads still present.	32
3.3	PCL:GEL fibers with the right morphology.	33
3.4	The deposition of PEO fibers is spiral	34
3.5	PEO Spray.	34
3.6	PEO Spray decrease but still present.	35
3.7	Stable electrospinning of PEO fibers.	35
3.8	PEO solution at 20%.	36
3.9	PEO solution at 15%.	36
3.10	PEO solution at 10%.	37
3.11	Similar deposition width with the higher caliber G16 needle as with the smaller G21.	37
3.12	G1 granulometry crystals.	38
3.13	G2 granulometry crystals.	39
3.14	G3 granulometry crystals.	39
3.15	G4 granulometry crystals.	40
3.16	Profile picture of the experimental arrangement, where we can see the PEO needle (left) raised 10 cm in relation to the collector.	40
3.17	Seringe with the PEO solution with the porogenic agent inside and a magnet.	41
3.18	G4 dissected crystal from a scaffold with the right size.	41
3.19	Another G4 dissected crystal with similar size.	42
3.20	PEO fibers with two G4 crystals electrospun on a glass slide.	42
3.21	PCL:GEL matrix after electrospinning.	43
3.22	PCL:GEL	44
3.23	PEO fibers around G2 crystals.	44
3.24	PEO fibers around G4 crystals.	45
3.25	PEO fibers around G2 crystals.	45
3.26	PEO fibers around G4 crystals.	46
3.27	PCL:GEL + PEO/G4 (x100 magnification)	46
3.28	PCL:GEL + PEO/G4 (x500 magnification)	47
3.29	PCL:GEL + PEO/G4 (x100 magnification)	47
3.30	PCL:GEL + PCL:GEL + PEO/G4 (x5000 magnification), after washing and crosslinked	47
3.31	PCL:GEL + PCL:GEL + PEO/G4 (x1000 magnification), after washing and crosslinked	48
3.32	PCL:GEL + PCL:GEL + PEO/G4 (x5000 magnification), after washing and not crosslinked	48
3.33	PCL:GEL + PCL:GEL + PEO/G4 (x1000 magnification), after washing and not crosslinked	48
3.34	PCL:GEL + PCL:GEL + PEO/G4 (x6000 magnification), after washing and crosslinked	49

3.35 PCL:GEL mass loss for the different crosslinking times. Where B is mass loss in percentage, (C) is the initial mass, and (D) is the final mass.	50
3.36 PCL:GEL scaffold with the four characteristic peaks of gelatin represented. .	51
3.37 ATR-FTIR absorbance spectrum for different crosslinking times.	52
3.38 PCL with Rhodamine B irradiated with green light.	53
3.39 PEO with Fluorescein irradiated with blue light.	53
3.40 PCL and PEO fibers deposition. The PCL fibers in orange and the PEO fibers in green are clearly visible in this image.	54
3.41 In this image is clearly visible that only PCL fibers are present. It is also noticeable the yellowish color present on the fibers due to PCL contamination with fluoresceins residues during PEO dissolution.	54
3.42 The aspect of dry samples.	55
3.43 Stress-Strain curve graphs.	59
3.44 The 24 hours and 12 days cell culture viability assay of the six different scaffolds.	60
3.45 DAPI assay of the 12 days cell culture with the general cells distribution on the surface of the samples.	60

LIST OF TABLES

2.1	PCL:GEL solution composition.	13
2.2	PEO solutions composition.	14
3.1	Amida I and Amida II FTIR intensities absorbance table for the PCL:GEL scaffolds different crosslinking times.	52
3.2	The ratio between Amida I and Amida II relative absorbance intensities, for the PCL:GEL scaffolds different crosslinking times.	52
3.3	Tensile tests data results.	56

ACRONYMS

DAPI	4',6-diamidino-2-phenylindole
DMEM	Dulbecco's Modified Eagle Medium
DNA	Deoxyribonucleic acid
ECM	Extracellular matrix
EW	Evanescent wave
FBS	Fetal bovine serum
FDA	Food and drug Administration
FTIR	Fourier infrared spectroscopy
GAGs	Glycosaminoglycans
GEL	Gelatin
GREAT	Group Research Engineering and Tissues
GTA	Glutaraldehyde
HA	Hyaluronic acid
HFFF2	Human caucasian foetal foreskin fibroblast
IR	Infrared
MSCs	Mesenchymal stem cells
NAD	Nicotinamide adenine and dinucleotide
PCL	Polycaprolactone
PDA	Paraformaldehyde
PEG	Polyethylene glycol
PEO	Polyethylene oxide

ACRONYMS

PLGA Poly(lactic-co-glycolic acid)

RGD Arginine-glycine-aspartate

SEM Scanning electron microscopy

UTS Ultimate tensile stress

UV Ultraviolet

*

INTRODUCTION

1.1 Contextualization

Tissue Engineering has emerged with the aim of making it possible to regenerate tissues or organs through the development of synthetic substitutes, consequently seeking to provide a new approach to conventional transplantation, either autologous or allogeneic, which are very limited solutions as they are dependent on the existence of an organ or tissue donor. It is also possible to circumvent certain biological barriers, such as rejection by the immune system through the use of biodegradable and biocompatible biomaterials and autologous or non-immunogenic cells [1]. An essential requirement is to create mechanisms of regeneration, instead of repair mechanisms in response to a wound [16].

There has been a great advance in Tissue Engineering through the development of several techniques for the production of new matrices [16]. Specifically, in the last two decades, much has been made on the electrospinning technique. This technique allows the production of matrices composed of fibers of diameters with dimensions ranging from nanometers to micrometers [5]. These matrices allowed the appearance of new substitutes for the most diverse tissues or organs because the fibers produced by electrospinning from biocompatible and biodegradable materials are good promoters of adhesion, proliferation and cell maturation [15]. Its fibers with small dimensions are similar to the native extracellular matrix, giving support and cellular organization, essential to the regeneration of the tissues [3]. However, the conventional electrospinning technique produces non-woven fibers which are deposited along a disorganized and non-oriented surface in the form of a densely packed network. This gives the matrices impermeability to cell infiltration because the distances between the fibers are much reduced and much smaller than the average cell size. The result are matrices that behave as two-dimensional structures where cells only adhere and proliferate along the surface. The low capacity of cellular

infiltration inside a matrix represents a challenge for Tissue Engineering, as the production of substitutes by electrospinning is concerned [16]. There is a consensus that larger pores and a high porosity are required for tissue growth and regeneration. However, the implementation of these characteristics has direct implications on the mechanical resistance of the matrices. A compromise between mechanical properties, pore size and porosity is fundamental in order to create a substitute capable of promoting good cell migration and the efficient diffusion of macromolecules which are indispensable properties for the growth and regeneration of tissues and organs while retaining adequate mechanical properties [32]. Consequently, several approaches, such as the development or combination of different techniques that promote cell infiltration in matrices produced by electrospinning have already been developed or are being studied [34].

In this context, the objective of this work is the development and characterization of a new three-dimensional (3D) porous matrix produced by electrospinning, which promotes an efficient cellular migration to its interior.

1.2 Framework

1.2.1 Extra Cellular Matrix

The extracellular matrix (ECM) constituent of all animal tissues comprises two different classes of macromolecules: (1) glycosaminoglycans (GAGs) and (2) fibrous proteins (collagen, elastin, fibronectin, and laminin). Most GAGs form covalent bonds with proteins secreted by cells, forming proteoglycans. These molecules form an anionic and hydrophilic substance with a gel behavior that provides compliancy and compressive strength to tissues, while allowing a good diffusion between blood and cells of oxygen, nutrients, metabolites, hormones, and cell debris [HynesRO.2009]. It is in this gel, commonly called the "fundamental substance", that the fibrous proteins, that provide tensile strength and structural support to the tissues are embedded [Kumbar2008]. In addition, fibrous proteins such as laminin and fibronectin play an essential role in cell adhesion because they have anchoring sites for the integrins. The different relative amounts of macromolecules in the ECM result from this being produced and oriented by the constituent cells themselves. We can highlight fibroblasts that secrete connective tissue ECM macromolecules, cartilage chondroblasts, and bone osteoblasts [HynesRO.2009].

The ECM is responsible for cell adhesion, migration, and proliferation, as well as support the regulation of cellular activity as it is a reservoir of hormones, growth factors, and intercellular communication medium [43].

1.2.2 Pore Size and Porosity

The matrix architecture has a significant impact on tissue regeneration [17]. Pore shape and size play an important role in matrix permeability with direct implication on cell migration, while porosity represents the percentage of void space available within the

matrix for cell growth. Previous studies have confirmed that thinner fibers promote cell adhesion and viability, and larger pores facilitate proliferation. However, too fine fibers and too large pores can mechanically compromise the substitute for possible in vitro or in vivo use. For the case of a matrix conventionally produced by electro-spinning the compromise exists between these two properties, where fibers with smaller diameters allow a more compact deposition with a smaller distance between fibers, resulting in a smaller pore size - and the inverse - thicker fibers result in less compact depositions with larger pore sizes. All together the resulting density is identical, with the pore volumes increasing to keep up with the increase in mass per volume that results from the bigger fibers diameters. There is also the notion that huge pore size causes the cells inside the matrix to fail to create multiple adhesions around them, being stretched along the inner surface of the pore thereby losing the properties that give it the intended 3D environment [19, 24].

No less important for the architecture of the matrices is the interconnectivity between the pores, so as to allow the vascularization and infiltration of the cells throughout the entire substitute. If there is no sufficient interconnectivity with sufficiently large channels for good cellular infiltration, there will be pores inaccessible to the cells inside the matrix [7]. Typically, there is no problem of interconnectivity between pores in conventionally electrospun matrices due to the inherent morphology of the 3D structure of non-oriented fibers, which results in pores with polygonal geometry, however, the very small distance that exists between the fibers functions as a resistance to cell migration [44].

The knowledge of how the alteration of these parameters affects cellular regeneration and the development of techniques and materials that allow the precise control of these parameters are important challenges to be overcome by Tissue Engineering in order to be able to develop substitutes that allow a complete and rapid tissue regeneration [25].

1.2.3 3D Scaffolds Production Techniques

The production of 3D substitutes that promote good cellular infiltration is currently an important challenge for Tissue Engineering [7]. Through several processes, it is possible to change the different structural properties of the matrices, such as pore size, porosity, and interconnectivity between pores. Each of the existing techniques currently has its pros and cons with a direct implication in infiltration distance [5]. However, the solution rather than the use of a single technique may result from a combination of two or more techniques [37]. There are numerous different approaches to making 3D arrays by electrospinning [25]. For the scope of this work two techniques will be used to promote cell infiltration: (1) leaching of a porogenic agent and (2) use of sacrificial fibers [27].

1.2.4 Leaching of a Porogenic Agent

Salt leaching is a technique that allows the production of 3D porous matrices. This technique was first demonstrated by Mikos et al. in 1994, in the development of highly porous

biodegradable polymer membranes through the use of a salt as a porogenic agent [30]. This technique involves the use of a polymer solution uniformly mixed with a porogenic agent, which upon evaporation of the solvent during the electrospinning process, results in a matrix composed of a polymer and porogenic agent [12]. The matrix is subsequently submerged in water for a given period of time, for the dissolution of the porogenic agent. These porogenic agents, when removed, create voids (pores) of different dimensions within the matrix [21, 39]. The size of these pores can be controlled by the particle size of the porogenic agent used. This technique is very effective for controlling pore size and increasing porosity. However, the interconnectivity between the pores resulting from the use of this approach is very random, not guaranteeing per se the ideal cellular permeability in the substitute [[Hutmacher2008, Onen2017], 30].

1.2.5 Use of Sacrificial Fibers

The concept behind the use of sacrificial fibers is very similar to the leaching technique of a porogenic agent. It consists of the electrospinning of a hybrid matrix composed of two polymers [41]. A water-soluble polymer - for example, poly (ethylene oxide) - to be further dissolved and another water-stable polymer, such as poly (ϵ -caprolactone) [13]. The electrospinning of the two polymer solutions simultaneously leads to the creation of a matrix of interlaced fibers which, by subsequent dissolution of polyethylene oxide, results in a less dense material with higher porosity and a larger pore size than a matrix produced by conventional electro-spinning. Via varying the ratio between the two polymers, we can control different mechanical properties of the matrix, such as pore size and porosity [44]. Unlike the leaching technique of a porogenic agent, this technique is not very accurate in controlling pore size, since the distance between the fibers will randomly depend on their deposition during the electro-spinning process and subsequent dissolution of the sacrificial fibers [4].

1.2.6 Electrospinning

Electrospinning is a technique that allows the production of scaffolds through the manufacture of continuous fibers with diameters of dimensions ranging from the order of nanometers to a few micrometers [13]. This apparently simple technique depends on several factors. Fibers characteristics such as their diameters will depend on various parameters, such as the physicochemical properties of the polymers and solvents employed, ambient temperature and humidity, the flow rate of the solution and the distance between the collector and the applied voltage on the syringe needle [13, 23]. However, after the determination of all the parameters for the production of a given matrix, electrospinning proves to be an inexpensive technique, and without the use of too sophisticated equipment, that allows the production of matrices efficiently and with excellent repeatability [15]. In the conventional electrospinning process, a polymer solution is pumped through a needle that has a diameter in the order of tenths of a millimeter. The metallic

and conductive needle also serves as an electrode, where a high voltage is applied (Figure 1.1). The applied high voltage creates an electric field around 100 kV/m between the needle and the grounded collector, which in laboratory models is usually 10 - 25 cm away from the needle [31].

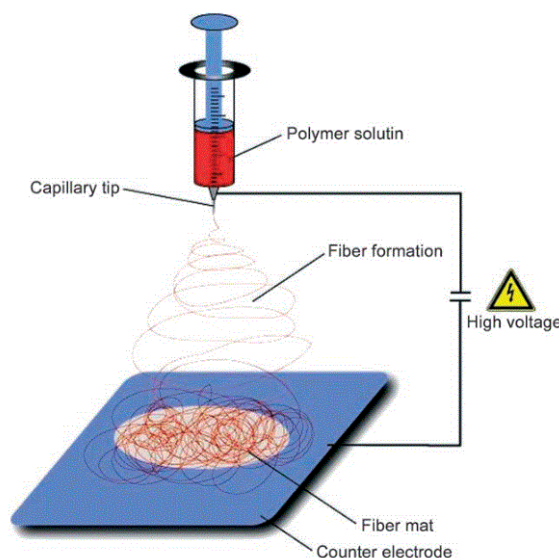


Figure 1.1: A typical arrangement of the electro-spinning technique. In this particular case, with a vertical axis arrangement of the electrodes [11].

Due to the applied electric field, the solution drop formed at the tip of the needle by the infusion pump is drawn into the shape of a cone having an angle of approximately 30° - it is named the Taylor cone (Figure 1.2). While the jet travels between the needle and the collector, the fibers become narrower due to the repulsion between the electric charges carried by the solution, the solvent evaporates and, if the electric field is strong enough, the solution jet will precipitate in the collector in the form of fibers while undergoing up to a 5 order magnitude diameter reduction [31]. Gravity and aerodynamics present little effect, when compared to the electromagnetic forces applied through tension, as a result of that, electrospinning can be performed either on a vertical or horizontal axis. Although a horizontal axis approach was used in this project, the vertical axis assembly is illustrated in this chapter [9, 33].

1.3 State of Art

The following bibliographic review presents the advances that have been achieved to date and reported in the literature, in order to provide the nanofibre membranes with pores of dimensions and interconnectivity suitable for the cellular migration to their interior.

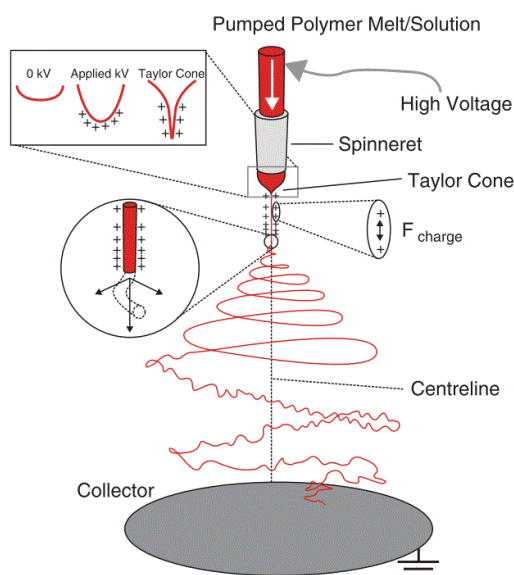


Figure 1.2: Electrospinning of a polymer and formation of the Taylor cone due to the accumulation of charges to the surface of the solution in the presence of an electric field.

1.3.1 Reference of the Use of Porogenic Agents

Plikk et al. have demonstrated that it is possible to produce matrices with complex porous structures (eg. tubular formations) using the salt leaching technique. By altering the shape, size and quantity of porogenic agent used it is possible to effectively control the porosity of the matrix. With the use of sodium chloride (NaCl) as a porogen, it was possible to obtain mechanically resistant matrices, with porosities around 93% [29].

In 2008, Kim et al. produced a three-dimensional porous matrix by electrospinning of hyaluronic acid (HA) nanofibers and collagen in combination with the salt leaching technique. In this approach, the salt particles were sieved over the deposited nanofibers during the electrospinning process [18](Figure 1.3).

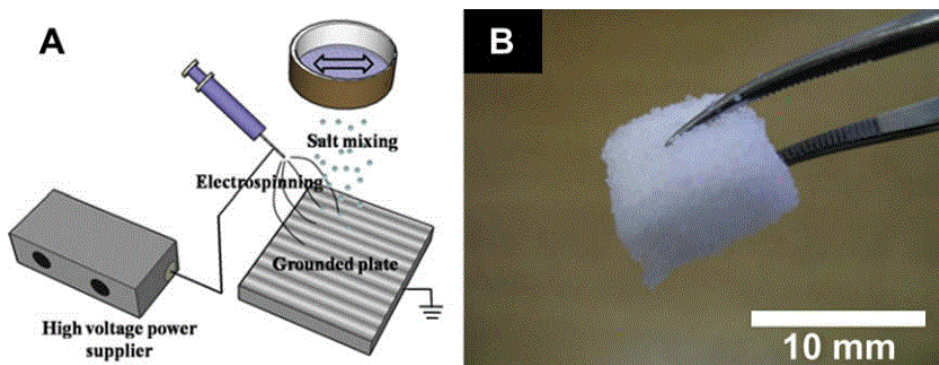


Figure 1.3: Technique for the use of porogenic agents. (A) Schematic, with the electrospinning process and the porogen being sifted over the electrospun scaffold. (B) Photograph of the resulting porous matrix [18].

In 2009, Wang et al. developed a new method to prepare porous matrices using the salt leaching technique (Figure 1.4. In this method, the porogenic agent composed of nanoparticles of salt was added directly to a polymer solution of PCL. With the aid of ultrasound, they obtained a solution with salt and polymer they were able to electrospin. Therefore, the porogenic agent was incorporated directly into the nano matrix fibers during the electrospinning process [36]. As can be seen in figure, Wang et al. detected the formation of salt aggregates in the solution even after the ultrasound, which resulted in the appearance of larger and poorly distributed pores [36].

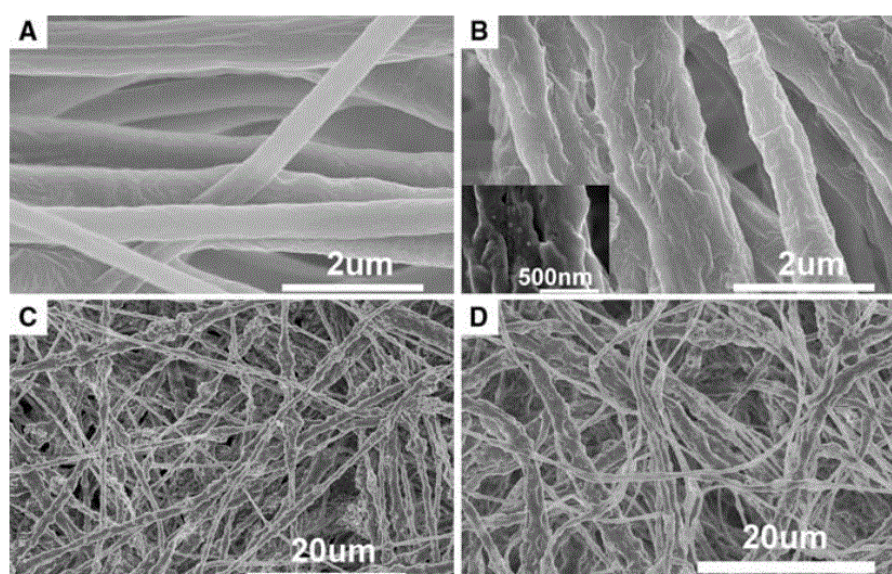


Figure 1.4: SEM images of: (A) non-porous PCL fibers; (B) surface morphology of a porous PCL matrix; (C) matrix before salt leaching; (D) matrix after saltleaching. [36]

They concluded that the uniform distribution of the salts in the solution and their stability throughout the entire manufacturing process are fundamental requirements for the efficient production of a porous matrix by electrospinning [36].

1.3.1.1 Sucrose as a Porogenic Agent

This technique is known as salt leaching because salts are commonly used as porogenic agents, but the use of ammonium chloride, gelatin, paraffin, and sucrose or glucose are also documented [30].

Dorati et al. in 2009 analyzed the effect of sucrose as a porogenic agent on the mechanical, physicochemical and structural properties of a polymer matrix. They determined that the porogen choice has direct implication in the three-dimensional structure (pore size, porosity, density, and mechanical properties) and physicochemical structure of the matrix. The use of cubic sucrose crystals gave rise to pores also having a cubic shape, thus confirming that the shape of the porogenic agent has a consequence in pore form. The sucrose gave rise to a matrix with larger pore size, higher porosity, and lower density compared to another matrix produced with the usual NaCl as porogenic agent [8].

Scaffold #	Porogen	Apparent density (g/L) ^a	Porosity (%) ^a	Pore size (μm) ^b	Compressive modulus (MPa)	Yield strength (MPa)
1	NaCl	0.12 ± 0.03	83.77 ± 0.62	200–300	3.66	0.4
2	Sucrose	0.088 ± 0.01	89.44 ± 0.4	200–600	2.43	0.22

^a Determined by displacement method (solvent – ethanol).

^b Determined by SEM.

Figure 1.5: Density, porosity and pore size of PLGA matrices prepared using two different porogen agents (NaCl or Sucrose) [8].

The larger pore size which was revealed by SEM analysis in the case of sucrose may have been caused by sucrose residues which had not been removed during the period in which the matrix was submerged in water for dissolution of the porogen, i.e. after this step the scaffolds were dried by lyophilization, which creates stress in the porous structure, sometimes leading to its destabilization and deformation. Dorati et al. state that the sucrose residues may have functioned as a cryoprotectant and thus have protected the fragile porous structure of the matrix, stabilizing its 3D architecture [8].

1.3.2 Reference to the Use of Sacrificial Fibers

Baker et al. described in 2007 the production of a hybrid matrix, where through the removal of sacrificial PEO fibers it was possible to increase the pore size and porosity of a PCL matrix manufactured by electrospinning. The matrices were fabricated by deposition of PCL and PEO aligned fibers simultaneously in the same collector, at a 60:40 PCL:PEO ratio, trying to ensure at all times the interlacing of the fibers. After electrospinning, the matrices were placed in water to dissolve the PEO fibers. The total removal of PEO with water was visually confirmed. The PCL and PEO fibers were doped with red and green fluorescent molecules respectively, and after removal of the sacrificial fibers with water the matrices were observed under a fluorescence microscope to confirm only the presence of the fibers doped with green fluorescent molecules. Mechanical tests were performed on the matrices after being submerged in water to remove the PEO and to non-submerged matrices in water for comparison of results. The mechanical tests detected a loss of mass of the order of 40% and only small deposits of PEO were detected. The tensile tests showed that the PCL + PEO matrices after the removal of the PEO fibers do not tolerate as much load which is indicative of a lower relative density of PCL, however the stress-strain curve is very similar to the curve of a matrix of pure PCL, with a reduction of Young's modulus [4].

To determine the influence of the removal of PEO fibers on cell infiltration, the matrices were seeded with mesenchymal stem cells (MSCs) for three weeks. At the end of the cell culture period, the matrices were cut crosswise and the mean transverse proliferation distance was measured by quantification of nuclear position by nuclear labeling with DAPI (4', 6-diamidino-2-phenylindole). Cellular infiltration assays were done on matrices with different quantities of the sacrificial component, and it was also demonstrated that an increase in PEO content improves cell infiltration. One limitation detected in this study, was that, although cell infiltration was improved it was not even through all the

scaffold volume. The best results obtained were with 60% sacrificial fiber removal, where about 45% of the cells remained at the outer quarter of the scaffold while only approximately 12% reached into the central quarter in a 200 μm thick scaffolds. However, this issue can possibly be addressed with a longer cell culture time, allowing cells to proliferate more evenly. Baker et al. demonstrated that it is possible to increase the permeability of the matrices produced by electrospinning, and thus to enhance cell infiltration through the removal of sacrificial components [4].

In 2009, Lowery et al. obtained similar results, also with a PCL + PEO hybrid matrix. Also in this study, the PEO functioned as a sacrificial component to increase pore and porosity of the PCL matrix. They concluded that matrix architecture has a major impact on cell growth and that porosity and pore size, in particular, have much influence on cell proliferation [25].

1.3.3 Reference to the Combination of a Porogenic Agent with Sacrificial Fibers

In 2013, Thadavirul et al. [35] used the combination of two techniques in the manufacture of a porous 3D matrix. They fabricated a hybrid matrix composed of a structural component of PCL and another sacrificial component of PEG with the addition of crystals of sodium chloride (NaCl) as a porogenic agent. This matrix was characterized and the data were compared with the properties of another PCL matrix treated only with NaCl and without PEG. They concluded that this hybrid matrix is more porous, has a larger pore size, and more interconnectivity between pores. The results also demonstrated that the PEG sacrificial component has a direct relationship with the morphological changes observed in the matrices. With the increase in molecular weight of PEG from 200 g/mol to 1000 g/mol, porosity and interconnectivity increased considerably. In vitro tests with bone cells revealed that the combination of the sacrificial part (PEG) with the porogenic agent (NaCl), resulted in substitutes capable of supporting cell proliferation and differentiation considerably better [35].

MATERIALS AND METHODS

2.1 Materials

2.1.1 Polycaprolactone

Poly (ϵ -caprolactone), (PCL) commonly referred to as polycaprolactone is a synthetic, aliphatic, biocompatible, and biodegradable polyester approved by the Food and Drug Administration (FDA) for use in humans [2, 20]. PCL, with molecular formula $(C_6H_{10}O_2)_n$, is synthesized by the polymerization of the ϵ -caprolactone monomer after the opening of its cyclic ring. The use of different catalysts for the catalytic reaction results in different molecular masses, different terminal groups and different chemical structures [10, 40]. PCL's average molecular weight ranges from 3,000 - 80,000 g/mol. It is a semi-crystalline polymer having a melting point between 59-64 °C and a glass transition temperature of -60 °C. The slow degradation of PCL in the physiological environment occurs in two stages: (1) hydrolysis of the ester bonds and (2) subsequent absorption and intracellular degradation of PCL fragments without cellular damage [2, 14].

Due to the rheological and viscoelastic properties of PCL, it is possible to it through the electrospinning process, for the production of micro/nano fibers for tissue engineering scaffolds [7].

PCL is also compatible with other polymers, allowing the creation of copolymers with different crystallinity, solubility and degradation time. These attributes make PCL a widely used material in the study of various pharmaceutical, medical and biomedical applications, such as slow drug delivery systems, prostheses, implants, biodegradable sutures, and tissue engineering scaffolds [38].

2.1.2 Gelatin

Gelatin is derived from collagen by controlled hydrolysis. It is a natural biopolymer and is highly efficient for the production of substitutes for use in Tissue Engineering [6]. Collagen is an important protein found in native ECM and potentiates cell proliferation [22]. It is one of the main components of connective tissues and is also found in the skin, tendons, cartilage, and bones. The collagen protein has, in its constitution, Arginine-Glycine-Aspartate (RGD) polypeptide sequences, which are anchor points to the RGD integrins present in cell membranes for cell adhesion. Gelatin, when used for electro-spinning, allows the production of micro/nanofiber scaffolds very similar to the native ECM [42].

Gelatin also has excellent biocompatibility and biodegradability. Some of its characteristics that allow gelatin to have these benefits are what makes it too hydrophilic and very hydro soluble. For this reason, gelatin or matrices with gelatin in their composition must be crosslinked to reduce their solubility [42].

2.1.3 Combination of PCL with Gelatin

PCL is a synthetic polymer with good mechanical properties, such as its elastic modulus and ductility, for use in the production of electrospun scaffolds. However, it does not have binding sites for integrins and is hydrophobic, which makes it a poor polymer for cell adhesion [42].

A matrix produced by combining PCL with a natural polymer such as gelatin is commonly used in Tissue Engineering. It is thus possible to combine the good mechanical characteristics of PCL with the beneficial ones of gelatin - the cell adhesion sequences [38].

Gelatin, when combined with PCL, leads to increased PCL hydrophilicity and also improves interaction between cells and the scaffold, which results in a better cell adhesion capacity of the hybrid matrix.

2.1.4 Polyethylene Oxide

Polyethylene oxide (PEO), also known as polyethylene glycol (PEG), has the chemical formula $C_{2n}H_{4n} + 2O_n + 1$. The term PEG is usually applied when the polymers have an average molecular mass of less than 20,000 g/mol while PEO for polymers with higher masses. PEO is a biocompatible, biologically inert, and soluble in water [26] and in many other solvents [11, 31].

2.2 Solutions

Concerning the production of the matrices, the PCL:GEL and PEO/sucrose polymeric solutions (PEO/sucrose, PEO fibers when added with sucrose) were first prepared. The polymers used were PCL (mean molecular weight $M_n = 80$ kg/mol), cold water fish skin

gelatin, and PEO (molecular mass $M_w = 100,000$ kDa). All polymers that were used were of the Sigma-Aldrich brand. Two solvents were purchased: (1) glacial acetic acid (99.7% purity, Fisher Chemical brand) for use with the PCL:GEL solution, and (2) chloroform stabilized with ethanol to be used in the solution of PEO, of the brand CARLO ERBA Reagents. The porogenic agent chosen to be added to the PEO solution was sucrose ($\rho = 1.59$ g/cm³, sugar of the Sidul brand) because it had a density similar to that of the chloroform solvent ($\rho = 1.49$ g/cm³). This way we can have a solution as homogenous as possible. Prior to the preparation of the solutions, chloroform had to be saturated with sucrose. This is to prevent dissolution of the porogen when it is added to the PEO solution. The PCL:GEL and PEO solutions were used individually, and also simultaneously for the production of the various matrices.

2.2.1 Preparation of Solutions

Three different solutions were prepared with the following compositions:

- A solution composed of PCL plus gelatin (PCL:GEL) polymers in equal proportions, dissolved in a solvent composed of glacial acetic acid and distilled water. This solution served to produce the main matrix, to which we want to enhance its cellular infiltration capacity. The composition of this solution was determined and is described by the author, MSc Luís Miguel Dias Martins.

Table 2.1: PCL:GEL solution composition.

Label	Composition
PCL:GEL	Solute - 20%
	PCL - 50%
	Gelatin - 50%
	Solvent - 80%
	Glacial acetic acid - 95%
	Distilled water - 5%

- The other solution prepared is composed of PEO at the 10% mass percentage dissolved in chloroform saturated with sucrose. This solution acts as a sacrificial and transport matrix for the porogen, and was used in combination with the PCL:GEL solution to obtain a hybrid matrix. It was designated by PEO/G#, where G# refers to the granulometry of the porogenic agent incorporated in the solution, which may have four different sizes: G1 = 0 to 50 μm ; G2 = 50 to 100 μm ; G3 = 100 to 150 μm ; and G4 = 150 to 200 μm . The concentration of porogenic agent was always 10% (w/w). When there was no incorporation of the porogenic agent the designation used was G0.
- A solution of 20% PCL dissolved in 95% acetic acid with 5% distilled water was also produced for fluorescence assays so that it was possible to determine the efficiency

Table 2.2: PEO solutions composition.

Label	Solute (%)	Solvent (%)	Porogen (μm)
	PEO	Chloroform	Sucrose
PEO/G#	10	90	G1 = 0 - 50 (10%.w/w)
			G2 = 50 - 100 (10%.w/w)
			G3 = 100 - 150 (10%.w/w)
			G4 = 150 - 200 (10%.w/w)

of the removal of PEO sacrificial fibers. Despite the autofluorescence of gelatin, it was not used because after the ultrasonic baths it lost its fluorescence properties. When Rhodamine B (a fluorescent compound used in the fluorescence assays) was added, the electrospinning jet became unstable, due to that a solution without gelatin in its composition was chosen.



(a) PCL:GEL.



(b) PEO.



(c) PCL.

Figure 2.1: Solutions aspect.

2.2.1.1 Production of Sucrose Crystals in Different Granulometry

Sugar is supplied in the form of crystals having sizes that range from approximately $50\text{ }\mu\text{m}$ up to about $500\text{ }\mu\text{m}$. Crystals were milled using a blender (Figure 2.2a), and subsequently graded using four sieves of the brand Analysensieb (Figure 2.2b). These sieves have nets with the following dimensions: $50\text{ }\mu\text{m}$; $100\text{ }\mu\text{m}$; $150\text{ }\mu\text{m}$ and $200\text{ }\mu\text{m}$. The sugar is placed on top of the $200\text{ }\mu\text{m}$ sieve, and the set of sieves is placed in an electric sieve shaker (model AS 200 of the Retsch brand). This equipment generates a throwing movement with three-dimensional angular momentum, which tosses the crystals evenly over the entire surface of the sieves. The selected vibration amplitude was 1.20 mm during 15-minute cycles. The crystals obtained were placed in flasks identified with their dimensions and closed to avoid moisture absorption by the sugar. Prior to grinding the sugar package was vacuum packed in a desiccator overnight to remove moisture and prevent the formation of agglomerates.



(a) Blender.



(b) Sieves shaker.

Figure 2.2: Equipment utilized to mill and grade the sucrose crystals.

2.2.1.2 Procedures for the Production of Solutions

To produce the PCL:GEL and PCL solutions, the following procedure was followed. Taking into account the quantities already mentioned, the reactants were added in the following order: first the water; then the glacial acetic acid; and finally the polymers. The solutions prepared were placed on a magnetic stirrer until the following day to dissolve the polymers. To help ensure good dissolution of the polymers in a short time, it is desirable to avoid dispersion of polymer on the walls of the flask. This was accomplished by placing the magnet prior to the addition of the polymers in the solvent, and setting a slow rotational speed of the magnetic stirrer. To ensure complete dissolution of the polymers, even from small clumps not visible to the naked eye, the solutions are sonicated for about 3 hours for the PCL:GEL solution, and about 1 hour for the PCL solution. With this, we avoid that small beads and fibers with non-uniform diameters are formed during the

electrospinning process. To avoid degradation of the polymers, these solutions should be used up to a maximum of 48 hours after they have been produced.

To produce the PEO/G# solution, the following procedure was followed. Taking into account the quantities already mentioned, the reactants were added in the following order: chloroform first and then PEO. The solution prepared was placed on a magnetic stirrer overnight to dissolve the polymer. The next day it was possible to use the solution without any further treatment. From the PEO solution flask, just before electrospinning, a known amount of solution was withdrawn to another flask (also with a magnet) and the porogen was added in the granulometry and desired amount. As in the grinding process, prior to the use of the porogen in the solution, the grains of the desired granulometry were placed under vacuum in a desiccator overnight to remove residual moisture and prevent the formation of agglomerates, also facilitating their weighing. The solution with the porogenic agent was placed on the magnetic stirrer until the grains dispersed evenly.

2.3 Scaffold Production

2.3.1 Experimental Arrangement

The same experimental set-up and parameters were used for the production of all the different matrices (Figure 2.3). Individual PCL:GEL and PEO depositions were also made for comparison of the electrospinning parameters, scaffolds properties and improvement of the solutions.

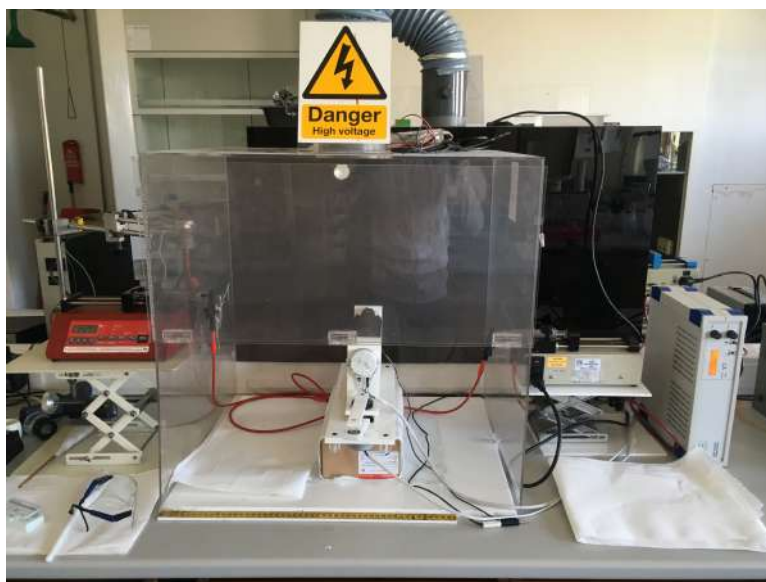


Figure 2.3: Experimental Arrangement.

The PEO/G# solutions are placed in 10 ml glass syringes due to the use of chloroform as the solvent. A G16 metal needle is attached to the syringe.

For PCL:GEL and PCL solutions, plastic syringes were used with an attached G21 metal needle.

The syringes with the solutions are placed perpendicular and on opposite sides of the anode (mandrel). The syringe with PCL:GEL or PCL is at the same height as the collector, while the syringe with PEO must be 10 cm higher than the collector.

Both components are mounted on a digital infusion pump and the following parameters are inserted: solution flow rate and syringe diameter. The infusion pumps used were two CHEMYX model Fusion100. To generate the electric field between the needle and the collector, a high voltage source (built in GREAT) is used. With the aid of two cables with crocodiles, the high voltage is applied to the needles and the collector (also built in GREAT) connected to the ground. The collector used for the production of all matrices is a cylindrical collector (a.k.a. mandrel or anode). Normally, this collector would only be used for the production of PCL:GEL + PEO/sucrose hybrid matrices, but as it was the objective to make comparative essays among all the matrices produced, the same collector was always used. The mandrel has two electric motors, which allow two degrees of freedom: (1) rotation and (2) translation perpendicular to the needle, which allows the fiber deposition longitudinally throughout the collector.

The deposition of the fibers is done on aluminum foil lining the entire collector. The choice of aluminum foil rests on its properties (good electrically conductive and malleable) that allow covering the entire collector and at the same time define an equipotential over the entire mandrel's surface.

2.3.2 Eletrospinning Parameters

The parameters applied to the different solutions were optimized during the course of this work. Some of these parameters, especially those used in PCL and gelatin matrices, are the result of previous work done at GREAT.

The electrospinning of the matrices was always done at approximately 40% relative humidity and 22°C. These parameters were constantly analyzed by a sensor, of the brand Rotronic, model Hygrolog. The temperature adjustment was made using the air conditioning available in the laboratory, and the humidity with a humidifier placed inside the electrospinning chamber. Immediately after production, the matrices are placed in a desiccator for a minimum of two days for complete evaporation of the solvents, as seen in Figure 2.4.

PCL:GEL + PEO composite matrix with sucrose crystals

This hybrid matrix results from the deposition of two independent fibers. One of PCL:GEL and another of PEO in equal quantity. This deposition was designated by, **PCL:GEL + PEO/G#**.



Figure 2.4: Post-electrospun scaffold inside the desiccator.

Production Parameters:

- PCL:GEL - needle-collector distance: 24 cm; flow rate: 0.3 ml/h; high voltage: 16kV.
- PEO/G# - needle-collector distance: 30 cm; flow rate: 0.3 ml/h; high voltage: 16kV.

To obtain matrices of sufficient thickness to carry out cell infiltration tests, we must have depositions with a minimum thickness of about 100 μm . For this reason, 6h continuous depositions were made, both for the matrices that would be used in in vitro tests, and those used for characterization and mechanical tests. The deposition has an average width of 127 mm.

It is important to connect the PEO syringe infusion pump first. By first laying a layer of PEO on the aluminum foil, in the post-production stages such as washing, it is easier to remove the scaffold from the aluminum foil. In addition, after washing the matrices have morphologically symmetrical surfaces on both sides, otherwise, the surface against the aluminum foil would be flat.

PCL + PEO composite matrix

This hybrid scaffold also results from the deposition of two independent fibers. One of PCL and another of PEO in equal quantity. This type of deposition was done for the fluorescence labeling assay.

Production Parameters:

- PCL - needle-collector distance: 24 cm; flow rate: 0.3 ml/h; high voltage: 18kV.
- PEO - needle-collector distance: 30 cm; flow rate: 0.3 ml/h; high voltage: 18kV.

Because it has no gelatin in its constitution, there is no need to crosslink this scaffold.

2.3.3 Scaffold Crosslinking

The various tests carried out throughout this work imply that the matrices have to completely submerged for long periods of time. This is the case of washing for the removal of PEO sacrificial fibers and sucrose porogenic agent, to perform tensile tests and in vitro tests. Since the matrices produced are sometimes composed of gelatin, they have a high rate of degradation and solubility. It is therefore important to ensure that fibers containing gelatin retain their physicochemical properties and morphology.

The crosslinking process leads to the creation of new covalent bonds between the amine groups of the gelatin polymer chains. Therefore, during the crosslinking process, there is a shortening and hardening of the matrix. To avoid contraction of the gelatin, the matrices are fixed to a flat metal plate with clamps, as seen in Figure 2.5.



Figure 2.5: Scaffold fixed to a flat metal plate.

Inside a plastic container and together with the matrices, two crystallizers, each with approximately 15 ml of a 50% prewarmed solution of Merck KGaA glutaraldehyde (GTA) are placed. The GTA solution is used as supplied without any prior processing. The plastic container is hermetically sealed (Figure 2.6) and placed inside the oven at 37°C for 4 hours.

Due to the toxicity of GTA, after the crosslinking process, the matrices are allowed to stand in the chemical hood for 48h to allow excess GTA to evaporate. All manipulation of the matrices in this step was done inside the laminar flow chamber.

After this treatment, the matrices were stored until needed.



Figure 2.6: Crosslinking container with two crystallizers inside.

2.3.4 Scaffold Washing

The washing step serves to remove the PEO sacrificial fibers and the porogenic agent (sucrose crystals) which are present in the matrices. The washing also serves for the smooth removal of samples from the aluminum foil where they were collected without damaging fibers.

The matrices are cut into the formats and sizes necessary for the assays and placed in petri dishes in a 10 mg/l glycine solution during 3 days, renewing the solution every day. The glycine solution serves to react with any remaining GTA residue in the matrices, resulting from the cross-linking process. At the beginning of this step, when wetting the fibers, while using tweezers it is possible to safely remove the aluminum foil without damaging the fibers.

After the 3 days in submerged in a glycine bath, the matrices are ready to be used.

2.4 Scaffold Characterization

With the exception of the optimization phase of the electrospinning solutions and parameters, the characterization was done post glycine treatment.

2.4.1 Morphological Analysis

During the optimization of the solutions and the electrospinning parameters, an optical microscope (Nikon Eclipse LV100), was used to observe short-term depositions on glass slides. This optical microscope has a built-in camera that allows the photographic recording of the samples obtained. This way, it was possible to record the consequences of the

adjustments made, and thus, to continuously improve the whole process. This optical microscope also served as equipment for quality control during the electrospinning process of the final matrices.

After process optimization, the final products were visualized by Scanning Electronic Microscopy (SEM). SEM analysis was performed on the HITACHI TM3030 Plus + Quantax70 benchtop equipment at CENIMAT/I3N facilities.

SEM images made it possible to observe the quality of the PEO fibers, with and without the porogenic agent, and the hybrid matrices of PCL:GEL + PEO/G# and to make a visual comparison of the different samples. It also served as a visual analysis of the crosslinking process. SEM images were recorded at different magnifications and later analyzed using the software Fiji is Just ImageJ (open source Software), and the histogram for fiber diameter in Excel (Microsoft) and KaleidaGraph, version 4.5 (Synergy Software).

For the SEM observation, the samples were cut into small pieces and glued with carbon double-sided adhesive tape to a metallic disk that supports the samples and recorded their positions. The samples being polymeric, and having a low conductivity were coated with a 5 nm thick layer of Iridium by cathodic sputtering for a better final image (as seen in Figure 2.7).



Figure 2.7: Metallic discs with scaffold samples ready to be analyzed on SEM.

2.4.2 ATR-FTIR

Through Fourier Transform Infrared Spectroscopy (FTIR) we can determine which compounds are present in the samples. A beam of electromagnetic radiation excites the molecules by changing their vibrational states. The frequency of the absorbed radiation is characteristic of the molecular bonds, thereby allowing the chemical composition of the matrices produced to be confirmed and the crosslinking procedure to be analysed.

In conventional FTIR the beam is passed through the sample and traversed in the sensor located on the opposite side of the sample. In the ATR-FTIR analysis, an attenuated total reflection (ATR) module, consisting of a crystal with a refractive index greater than the sample, is mounted. The crystal diffracts the IR beam so that it is incident on the sample at a given angle. As a consequence, the beam reflects at least once in the sample. This reflection is called the EW (Evanescent Wave) which traverses the sample by penetrating it about 0.5 to 2 micrometers, depending on the beam's wavelength, the angle of incidence and the refractive indexes of both the sample and of the crystal. The EW wave on leaving the crystal is detected on the sensor on the same side as the IR beam source. With the ATR module, it is possible to observe thick samples (such as the matrices produced during this project) that with the conventional FTIR would be impossible, because the beam does not have the capacity to cross the samples directly from one side to the other.

The ATR-FTIR equipment used was the Thermo Scientific Nicolet 6700 FT-IR with the attached SMART iTR ATR module (Figure 2.8). This analysis was carried out at CENIMAT / I3N. The range of wave numbers used in the analysis of samples was 500 cm^{-1} to 4000 cm^{-1} .



Figure 2.8: ATR-FTIR equipment.

2.4.3 Mass Loss Assays

A mass loss test was performed to assess the efficacy of the crosslinking process by determining the amount of gelatin that is dissolved with distilled water. Comparing the mass loss of PCL:GEL matrices crosslinked for different amounts of time, it was possible to determine the duration of treatment time with GTA to which the electrospun matrices have to be subjected. Since PCL is hydrophobic, and the non-crosslinked gelatin is very

hydrophilic and poorly water resistant, it is important that the mass loss be the least possible.

For this assay three PCL:GEL matrices were produced, with a 6h continuous deposition time. Each of these matrices was cut transversely into five equal pieces. Of these five pieces, one was stored and the other four were each one placed to crosslink during different intervals: 1h; 2h; 3h; and 4h.

Fifteen glass vials were numbered, preheated to ensure there was no condensation inside the vials, and weighted without the cap. Three samples of each piece were placed in each vial for a given cross-linking time. Three flasks corresponded to non-crosslinked matrices, others three to 1 h of crosslinking, and the other flasks to 2h, 3h, and 4h respectively. With the samples inside, they were left in the oven at 37 °C overnight so as to ensure that the samples were free of moisture, and again weighed. After we know the weight of the dried samples and still with the aluminium foil, they are then submerged in ultrapure water, and placed on the shaker inside the oven at 37°C for 4 days, changing the water each day. The water is then withdrawn, and the samples allowed to dry in the oven at 45 °C for two days and again weighed with the flasks. Weighing must be done as quickly as possible, avoiding too much time with the samples out of the oven to avoid absorbing moisture from the air. After being weighed, the samples are washed out from the aluminium foil, which is dried in the oven and also weighed. The weight of the aluminium paper is subtracted from the final weight of the samples, and also subtracted from the weight of the dehydrated matrices on the first day corresponding to the initial weight of the PCL:GEL matrices. The subtraction of these two masses results in the mass loss value for each crosslinking time. Statistical analysis was done with Excel software (Microsoft) and KaleidaGraph, version 4.5 (Synergy Software).

The calculation of the mass loss was done according to the following equation 2.1:

$$\text{mass loss (\%)} = \frac{m_I - m_F}{m_I} \cdot 100\% \quad (2.1)$$

Where m_I is the mass of the sample before being submerged and m_F is the mass of the sample after being submerged. Note that, both to m_I and m_F we must subtract the corresponding mass of aluminum foil as previously described in this section.

2.4.4 Fluorescence Assays

To confirm the efficiency of the washing process in the removal of PEO sacrificial fibers, the fibers were doped with two fluorescent compounds. For this assay a PCL+PEO matrix was made, without gelatin. Rhodamine B at 0.001% w/w and 0.01% w/w Fluorescein were added to the solutions respectively (Figure 2.9). **Warning: Rhodamine B is toxic and therefore it is necessary to use face masks, goggles and two pairs of nitrile gloves because Rhodamine B is absorbed by polymers and can cross the gloves. The solutions after being used are stored for about two days in glass containers with chlorinated tap water for inactivation of rhodamine B.**

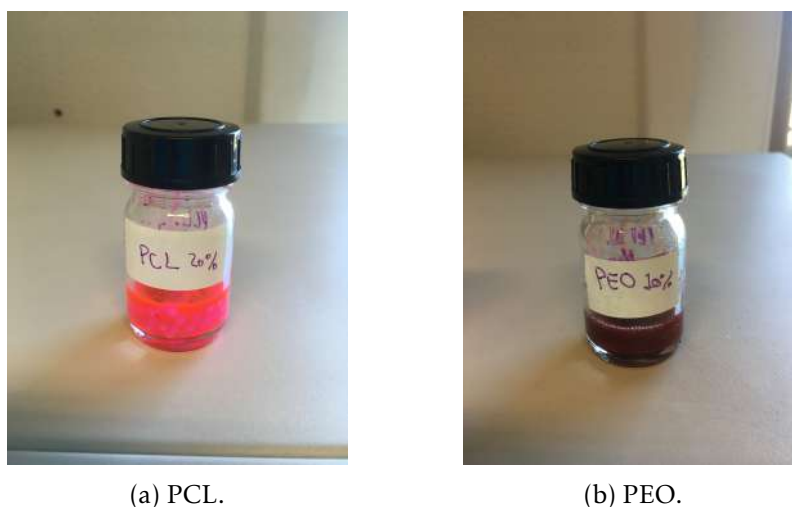


Figure 2.9: PCL and PEO solutions doped with Rhodamine B and Fluorescein respectively.

Then, the matrix was spun as described in the experimental procedures. During the electro-spinning process, glass slides were glued to the collector with tape-glue over the aluminum foil. Fibers were then collected on the glass slides for 1 min and subsequently observed at a magnification of 400x and 1 second exposure time on the Nikon Eclipse Ti-S epifluorescence microscope, equipped with a mercury discharge lamp and a Nikon D610 camera. Some of the glass slides with the samples previously to be observed under the microscope were washed for PEO fiber removal.

The acquired images were later analyzed and edited using Fiji software.

2.4.5 Tensile Tests

Traction assays were performed on the PCL:GEL individual deposition matrices and the hybrid matrices of PCL:GEL + PEO/G#. These tests served to assess some of the mechanical properties of the matrices, and how these properties vary according to the different solutions used. These tests, because they were always done under the same experimental conditions, allowed the comparison between the different matrices.

The equipment used is from Rheometric Scientific and controlled by MINIMAT software (P.L. Thermal Sciences, v1.60) with a 20N load cell.

For this assay 3 replicates of each of the following matrices were produced: PCL:GEL; and PCL:GEL + PEO/G#. The matrices were crosslinked and washed for removal of silver paper, sacrificial fibers, and porogen. Subsequently, each matrix was cut into five samples with the dimensions of 3x1 cm, and the samples were placed in Petri dishes identified with the type of matrix to which they correspond.

Tensile tests were performed on all hydrated samples, on a total of 90. The tests were done on the hydrated samples to approximate the test to the reality in which these matrices would be used, which is hydrated and in the physiological medium. In addition, being hydrated facilitates the experimental setup process, because matrices which contain



Figure 2.10: Sample being tractioned.

gelatin and have been cross-linked are very fragile when dry.

The tests were performed at an elongation rate of 5 mm/min. For each sample, the thickness and width were registered, as well as the initial distance (l_0) between the two clamps that hold the sample (Figure 2.10). The machine pulls the test pieces and the software collects information in real time on the applied force (F) and the elongation (Δl). With the data retrieved from the tensile tests, we can draw the stress-strain curves using the following equations 2.2 and 2.3:

$$\sigma = \frac{F}{A} \quad (2.2)$$

$$\varepsilon = \frac{\Delta l}{l_0} \quad (2.3)$$

For small stresses, the traction curve is linear and corresponds to the zone of the elastic behavior of the sample. The stress-strain relation in the elastic region is given by Hooke's law (see equation below 2.4), where E is the elastic constant, also called the Young's Modulus, which corresponds to the slope of the stress-strain curve in the elastic region.

$$\sigma = E \cdot \varepsilon \quad (2.4)$$

Since there are 90 tests, and a large amount of data to treat, an Excel file was used with a macro developed in GREAT, by Prof. Dr. José Ferreira, to directly obtain the values of

the Young's Moduli. The data obtained were statistically treated in Excel and the graphs were drawn on KaleidaGraph.

2.5 *In Vitro* Assays

Two cell assays were performed on the PCL:GEL and PCL:GEL + PEO/G# matrices. This step allows determining the ability of the matrices to promote cell adhesion, proliferation, and infiltration. By comparing the different matrices analyzed, it is also possible to know if the combination of selected techniques (salt leaching with sucrose and the use of sacrificial fibers) have resulted in the potentiation of cellular infiltration and if they do not have a negative influence on cell viability.

It is essential that all procedures relating to cellular assays occur in a sterile environment and that there is no contamination (bacterial, viral or fungal) of the cells, samples or solutions used. Any contamination hinders any reliable analysis of the results. To ensure sterility, all steps were performed inside a Level II microbiological safety chamber (Esco Labculture II) in the GREAT cell culture laboratory. All solutions and materials used were pre-sterilized in an autoclave and subjected to UV (ultraviolet) radiation inside the microbiological safety chamber.

The use of a clean lab coat, disposable gloves, and a surgical cap are required to avoid contamination by the user during procedures.

2.5.1 Preparation of Samples for Cell Culture

For the cell assays, 5 circular samples with 12mm diameter of the electrospun and crosslinked matrices of PCL:GEL and PCL:GEL + PEO/G# are cut out. For this, a metal punch and hammer are used.

The collected samples are taken into the microbiological safety chamber and submerged in 90% ethyl alcohol in pre-autoclaved glass Petri dishes. They are allowed to stand for 20 minutes. During this step, the aluminum foil is removed from the samples with the help of two sterile metal tweezers.

The samples are then submerged in a sterile glycine (10 mg/l) solution for three days to inactivate the GTA residues and removal of the sacrificial fibers of PEO and the porogenic agent (if they are present). This solution should be changed every day and whenever possible irradiate the materials with UV light. After this treatment, the samples are ready for use in the cell culture assays.

The samples were mounted on teflon supports and placed in 24-well plates as seen in Figure 2.11. The purpose of these teflon supports is to secure the matrices, preventing them from loosening or floating during cell assays. The exposed sample area is 0.5 cm².



Figure 2.11: Teflon supports mounted on a 24-well plate.

2.5.2 Cell Culture with the HFFF2 Cell Line

For in vitro assays, the adherent and non-tumor cell line HFFF2, which are human skin fibroblasts, was chosen. Cell lines have the advantage of being composed of a single cell type. This is advantageous for the validation of the experimental tests, in that we can better correlate the data obtained with the parameters tested, not increasing the entropy with factors that we can not control, such as different types of cells present with different biological behaviors. Non-tumor cell lines, however, have a limited number of cell divisions (about 30-40 mitosis) until they undergo senescence. HFFF2 were obtained from the European Collection of Authenticated Cell Cultures, UK.

Culture medium consisted of DMEM (Dulbecco's Modified Eagle's Medium, Sigma-Aldrich #D5030) supplemented with 1.0 g/L D-glucose (Gibco, #15023-021), 3.7 g/L sodium bicarbonate (Sigma-Aldrich, #S5761), 1% GlutaMAX™(L-alanyl-L-glutamine dipeptide, Life Technologies, #35050-038), 1% sodium pyruvate (Gibco, #11360039), penicillin (100U/ml) and streptomycin (100 µg/mL) (Invitrogen, #15140122), 10% FBS (Fetal Bovine Serum, Invitrogen, #10270106). To the culture medium were further added the following antibiotic amount: 20 µg/ml gentamicin.

Cells are allowed to proliferate on T25, placed in a Sanyo MCO19AIC (UV) incubator until they reach a confluence state of about 70% to 80% for seeding on the samples.

Seeding density was 30000 cells per cm². The two cell control wells in the culture dish were also seeded with the same cell density. The culture plates were left in the incubator for cells to adhere and proliferate. The culture medium was changed every three days or when cell viability assays were performed following the experimental protocol described next.

2.5.3 Cell Culture Viability Assays

Over the cell culture period, resazurin tests were performed regularly to quantify cell viability and thus obtain cell adhesion rates to matrices and proliferation. Resazurin is a blue dye that is metabolized by the cells and thus reduced to resorufin - the pink fluorescent compound.

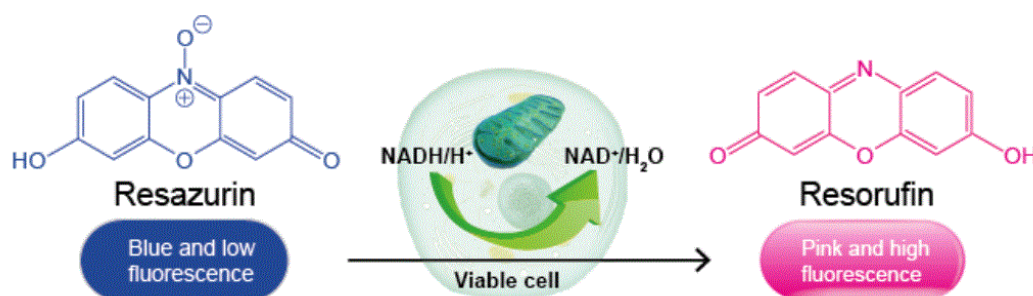


Figure 2.12: Schematic representation of the reduction of resazurin to resorufin by the enzyme NAD (nicotinamide adenine and dinucleotide) by metabolically active cells. [adapted from <http://file.bioutil.com/downloads/Vita-Blue-Cell-Viability-Reagent.pdf>]

The change in the color of the medium is proportional to the number of living. The variation is measured by reading the absorbance at 600 nm (absorption peak of resazurin) and at 570 nm (absorption peak of resorufin). Resazurin is not cytotoxic at the concentration used, which allows for cell analysis without compromising cell viability.

For this assay, a solution composed of resazurin at 0.04 mg/ml and complete culture medium was produced at a 1:1 (*v/v*) ratio. This solution was distributed into the culture wells in the following amounts: 200 μ l/well of solution in the sample wells; and 800 μ l/well of solution in the control wells. Cells were incubated for three hours with resazurin, after which the absorbance was read.

To read the absorbance, 130 μ l of the solution was withdrawn from each well as uniformly as possible and placed in a 96 well plate, as seen in Figure 2.13.

To read the absorbance, a Biotek ELx800 UV plate reader (Figure 2.14) was used, and the statistical treatment was done with Excel software.

2.5.4 Cell Culture Infiltration Assays

For the quantification of cellular infiltration, the nuclear labeling method with DAPI was used (Figure 2.15). DAPI binds strongly to DNA regions rich in Adenine and Thymine bases. When bound to DNA, it increases its fluorescence by a factor of approximately 20x, leaving the nuclei visible by epifluorescence microscopy.

This method involves cell fixation and is, therefore, the terminal step in the cell culture. The matrices will be removed after three to four weeks from the culture wells. Cells are fixed with paraformaldehyde (PFA). Fixed cells are labeled with DAPI and observed under the microscope. The side of the matrix where the seeding was done and

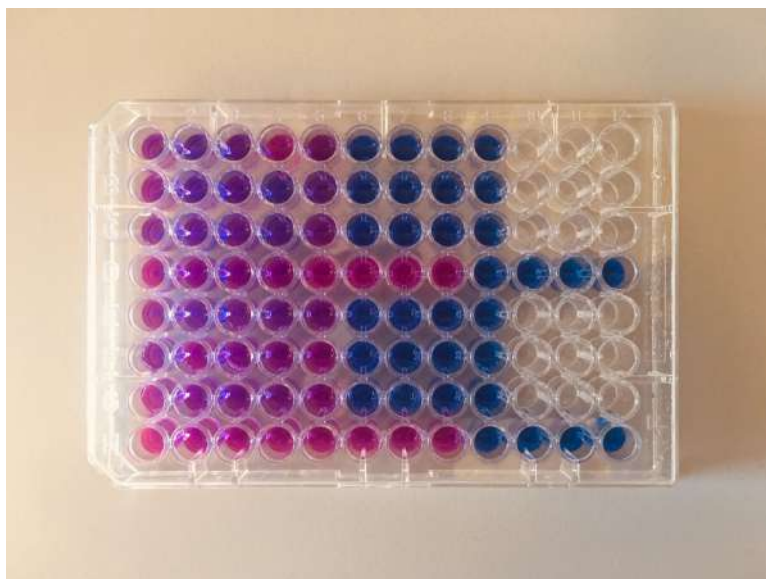


Figure 2.13: The 96 well plate ready to be analyzed.



Figure 2.14: The 96 well plate mounted on the UV absorbance plate reader.

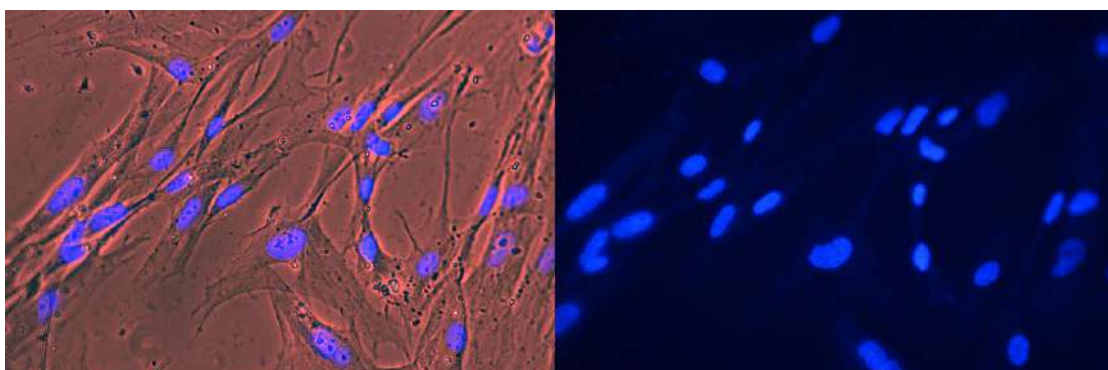


Figure 2.15: Nuclear labeling of cells with DAPI at GREAT cell culture laboratory.

then the opposite side is displayed. If cells on the opposite side are detected it is a good indication of the ability of the cells to traverse the matrices. These results were compared between the different matrices produced.

PRESENTATION AND DISCUSSION OF RESULTS

3.1 Determination of the Scaffolds Production Parameters

In order to successfully electrospinning the solutions used in this work, it is first necessary to study the parameters that guarantee a stable deposition of the different fibers with the desired morphology. The rigorous study of these parameters is also of great importance in order to be able to replicate the results later.

For the production of PCL:GEL + PEO/G# hybrid matrices with the different sizes of sugar crystals, PCL:GEL and PEO solutions were studied individually to facilitate the optimization of the different parameters and perception of how each parameter affects the quality of the fibers. The optimization of PEO went through three phases: (1) optimization of the production of PEO fibers per se, (2) confirmation of the structure and sizes of the crystals of sucrose used as porogenic agent and (3) check if the parameters applied in the electrospinning of PEO alone are good for the production of the PEO together with the porogenic agent and if the characteristics of the crystals are preserved after the deposition.

The literature reports the deposition of some of the solutions used and this information was used as a starting point for optimization. Throughout this study, data were recorded on the parameters of the solutions, such as polymer and solvent quantities, and ultrasound time (for the solutions with gelatin).

The following electrospinning parameters were also recorded: relative humidity; temperature; needle-collector distance; applied voltage; solution flow rate and needle gauge.

PCL:GEL fibers

The PCL:GEL solution had already been studied in a previous work at GREAT, that

was the beginning of the study of the parameters.

The same production parameters were applied for PCL:GEL solutions, as well as the same experimental setup.

In the early depositions, the formation of beads along the fibers was observed, as seen in Figure 3.1.

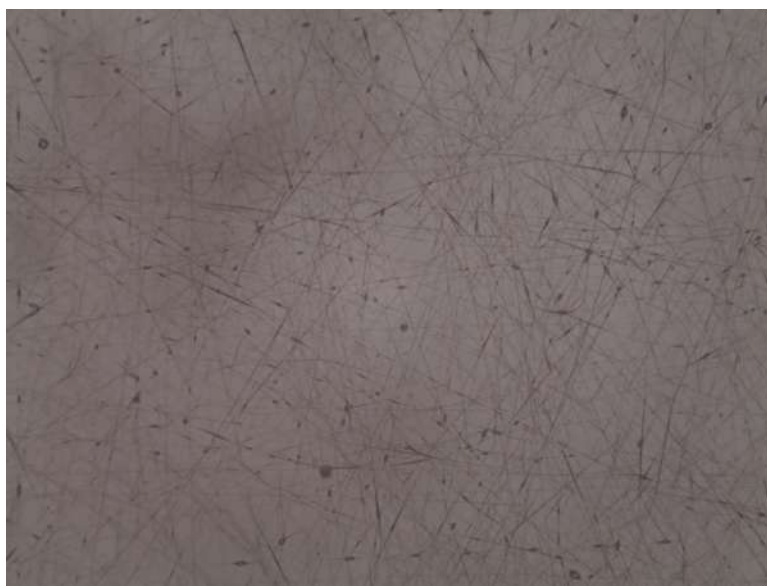


Figure 3.1: The formation of beads along the fibers.

In the first approach, the voltage was increased, from 16kV to 18kV. The fibers kept their general morphology, well stretched and did not tear. However, the formation of beads persisted (Figure 3.2).



Figure 3.2: Fibers with good morphology but with beads still present.

3.1. DETERMINATION OF THE SCAFFOLDS PRODUCTION PARAMETERS

Two new PCL and gelatin solutions were made. They were both placed in an ultrasound bath. The first one for another hour (4h of ultrasound) and the second the same 3h of ultrasound but paying attention to water temperature to avoid surpassing 45°C. Concerning this, the water was changed every 30 min.

The PCL:GEL solution that was subjected to 4 hours of ultrasound was impossible to electrospin. There was no jet and the needle was dripping the solution. This may be related to the degradation of the polymer chains of gelatin due to excessive heat during the ultrasound treatment.

The solution that was submitted to 3 hours of ultrasound with controlled temperature allowed the deposition of fibers with uniform diameters, without bead formation, and with excellent stability throughout the period during which electrospinning takes place (5 hours)(Figure 3.3).



Figure 3.3: PCL:GEL fibers with the right morphology.

It was thus confirmed that the parameters described in the literature were adequate for the electrospinning of PCL:GEL solutions.

PEO fibers

As the PEO fibers would later be electrospun together with those of PCL:GEL, a 16kV needle-collector potential difference was set. This way, it was possible to use a single voltage source.

PEO with a molecular weight of 100 kDa was chosen because polymeric solutions of high molecular mass generally give rise to thicker solutions, more difficult to electrospin and larger fiber diameters. In the following figure, it is possible to see a solution of PEO with 900 kDa at 2% in chloroform. Mention: the chloroform solvent is previously saturated with sucrose to avoid dissolution of the porogen when it is added to the solution.

We can observe that the deposition of the fibers is spiral. This type of deposition is not effective for deposition of sacrificial fibers (Figure 3.4).



Figure 3.4: The deposition of PEO fibers is spiral

With PEO of molecular mass of 100 kDa, it was first attempted to produce a 5% (w/w) solution in chloroform. The reason for starting with a solution at only 5% is because chloroform is a non-polar solvent, and therefore there may be some difficulty in drawing the fibers along the jet.

In this deposition, a solution spray was observed instead of continuous fibers. The distance from the needle to the collector was 20 cm (Figure 3.5).

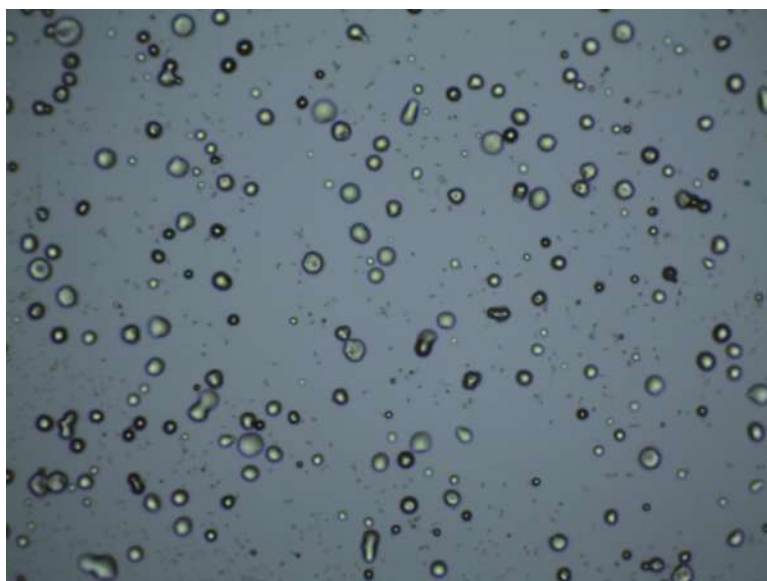


Figure 3.5: PEO Spray.

As the needle-collector distance was decreased, the spray was found to decrease, but

not altogether - drops of solvent and polymer were still observed in the deposition (Figure 3.6).

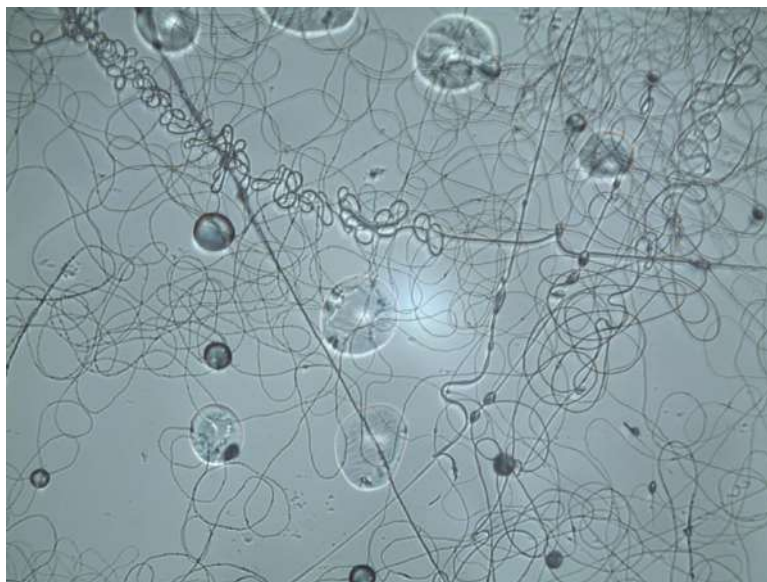


Figure 3.6: PEO Spray decrease but still present.

As it was not practical for the experimental assembly to continue to decrease the needle-collector distance, it was decided to increase the concentration of PEO in the solution and return the distance of 20 cm. Solutions of 10%, 15% and 20% (*w/w*) PEO in chloroform, two different needle sizes (21G and 16G), and two different flows (0.3 ml/h and 0.2 ml/h) were tested.

With these parameters it is possible to produce a stable jet, with no solvent spray and sufficiently uniform fibers for sacrificial fibers deposition (Figure 3.7).



Figure 3.7: Stable electrospinning of PEO fibers.

The major difference between the change of these parameters was the width of the deposition. In the depositions with 15% (Figure 3.8) and 20% PEO (Figure 3.9), the deposition had a maximum width of 55 mm and 28 mm respectively.

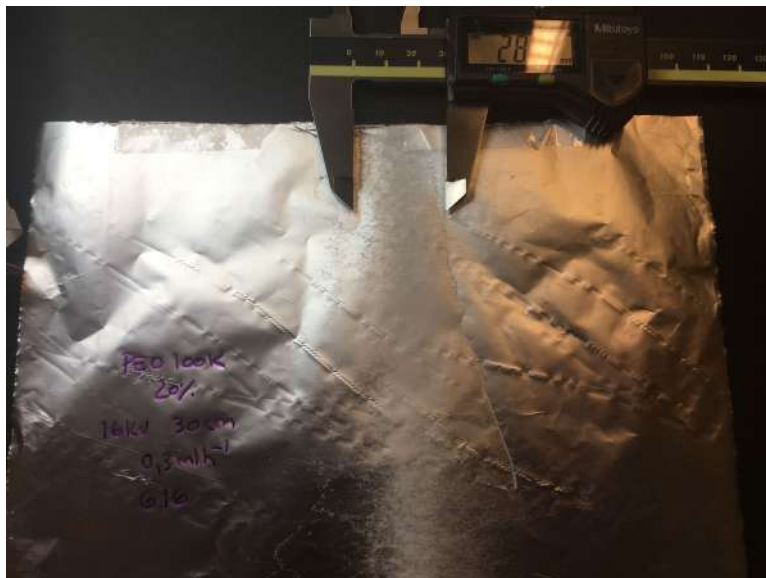


Figure 3.8: PEO solution at 20%.

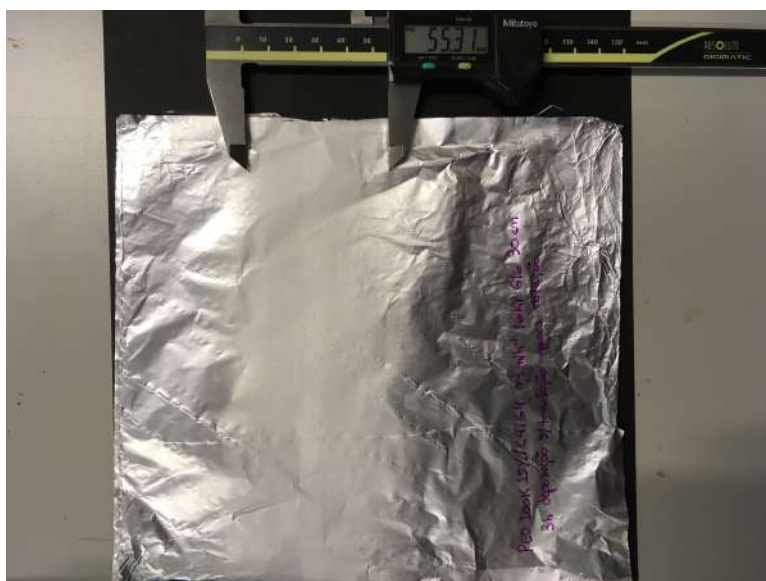


Figure 3.9: PEO solution at 15%.

While deposition with 10% PEO, a deposition of 127 mm width was possible (Figure 3.10).

The larger deposition width turned out to be a preferred factor. This is because the deposition of PCL:GEL covers the aluminum foil over the entire width, and it was desirable that the sacrificial fibers could be present in the largest possible deposition area. First, because it makes a scaffold with a mixture of fibers more uniform and secondly

3.1. DETERMINATION OF THE SCAFFOLDS PRODUCTION PARAMETERS

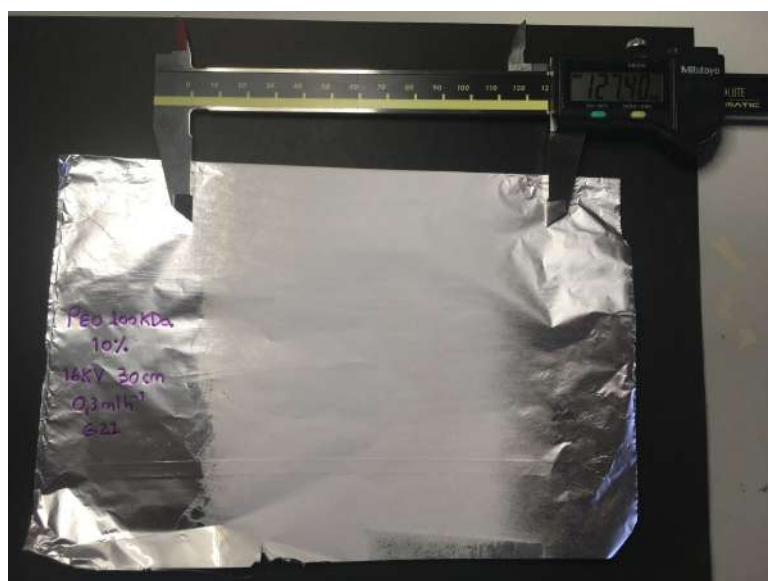


Figure 3.10: PEO solution at 10%.

because it has a larger deposition area available for the tests that were intended to be made to the matrices. During these depositions, it was found that the use of a larger gauge needle did not significantly alter the fiber deposition width (Figure 3.11).

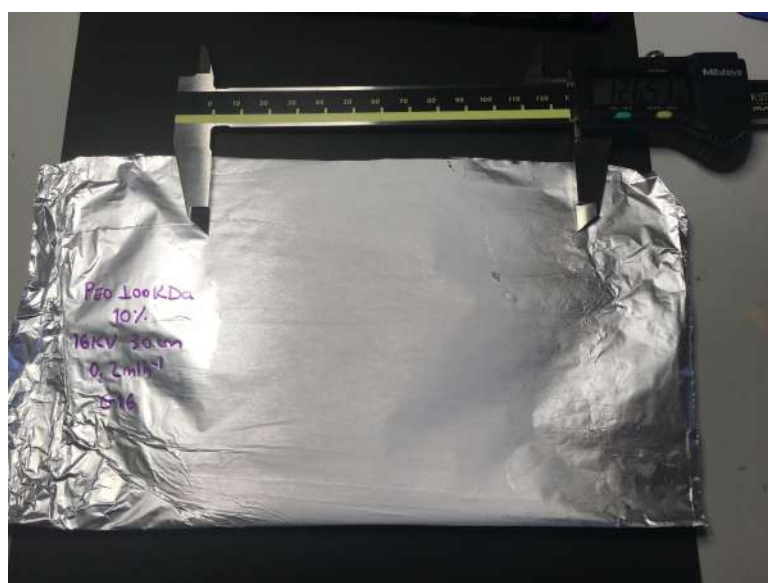


Figure 3.11: Similar deposition width with the higher caliber G16 needle as with the smaller G21.

The largest gauge needle (G16) was therefore chosen since it would have been necessary to have a gauge needle large enough to later be able to electrospin the fibers with the porogen without clogging.

Porogenic agent

Before incorporating the porogenic agent into the PEO solution, the best way to separate it in different granulometry was investigated.

Four sieves were used to separate the sugar crystals in the four different grades required ($G1 = 0$ to $50\ \mu\text{m}$, $G2 = 50$ to $100\ \mu\text{m}$, $G3 = 100$ to $150\ \mu\text{m}$, and $G4 = 150$ to $200\ \mu\text{m}$).

Separation by manual stirring of the sieves was found to be very slow and physically difficult to perform. To solve this problem was used an electric sieve shaker, and to accelerate the process was made the previous crushing of the sugar grains with an electric chopper. This increased the number of smaller grains, facilitating the separation process. To prevent the sugar grains from sticking together, they were sealed in hermetically sealed containers and under vacuum prior to use.

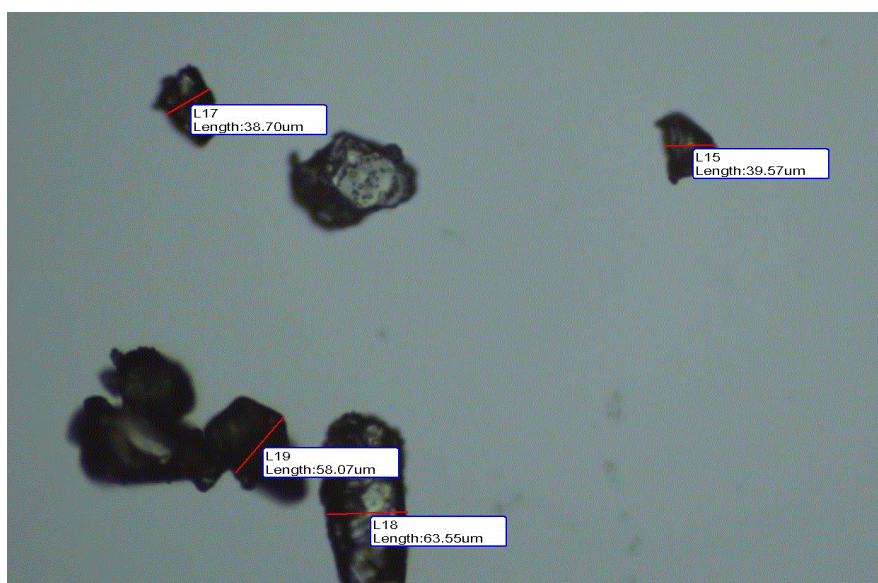


Figure 3.12: G1 granulometry crystals.

A good separation of the crystals in the different granulometries was observed (Figures: 3.12; 3.13; 3.14; 3.15). However, it was impossible to guarantee that there was no residual presence of some grains of other dimensions.

PEO fibers with the porogenic agent

The deposition of PEO with the porogenic agent was carried out. The purpose of this step was to ensure that after the addition of the porogenic agent to the solution, the fibers continued to be correctly electrospun, the needle did not clog and the crystals were not dissolved in the solution with the sucrose-saturated chloroform.

It was found that the electrospinning parameters were correct also to be used in the deposition with the crystals of sucrose, and that the fibers maintained their morphology.

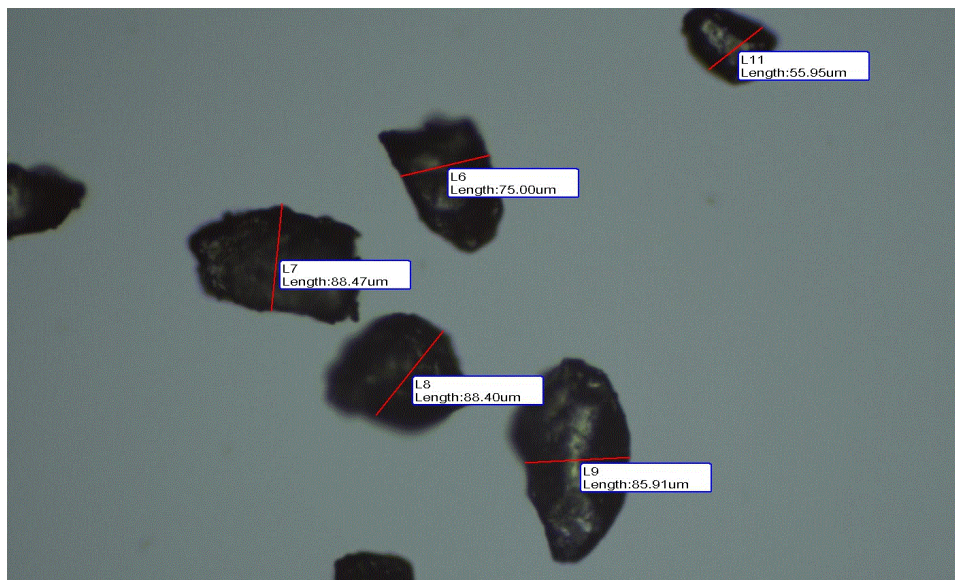


Figure 3.13: G2 granulometry crystals.

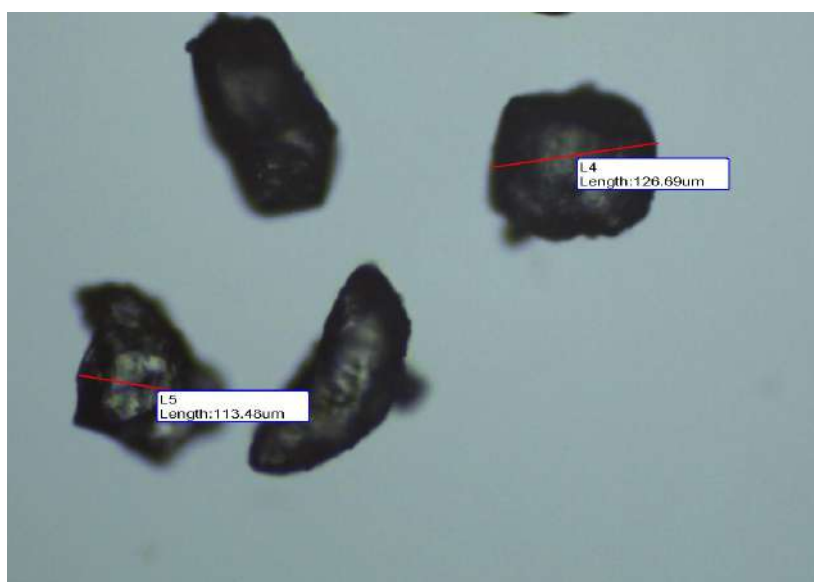


Figure 3.14: G3 granulometry crystals.

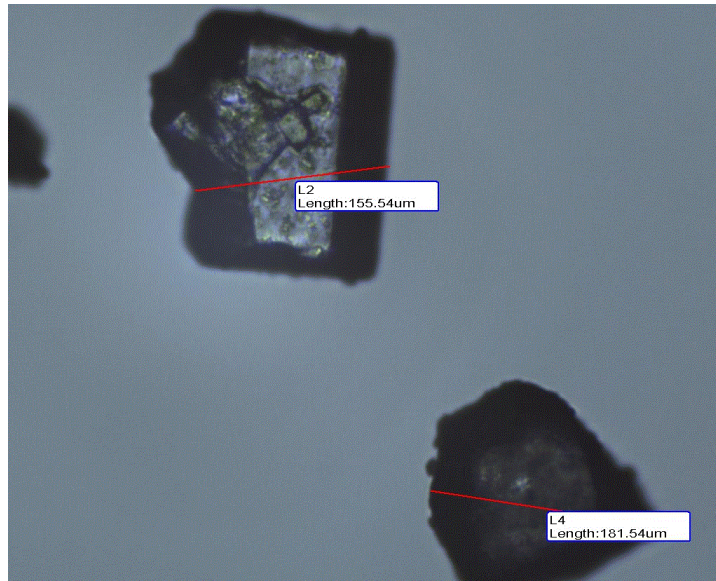


Figure 3.15: G4 granulometry crystals.

However, in the deposition, sugar grains were not detected in the amount that was expected. On closer inspection, it was found that the crystals, due to their mass, were released from the fibers along the path to the collector. To solve this problem the injection pump was placed 10cm higher than the collector (Figure 3.16). This solved the problem and the crystals were deposited in their entirety in the collector together with the fibers.

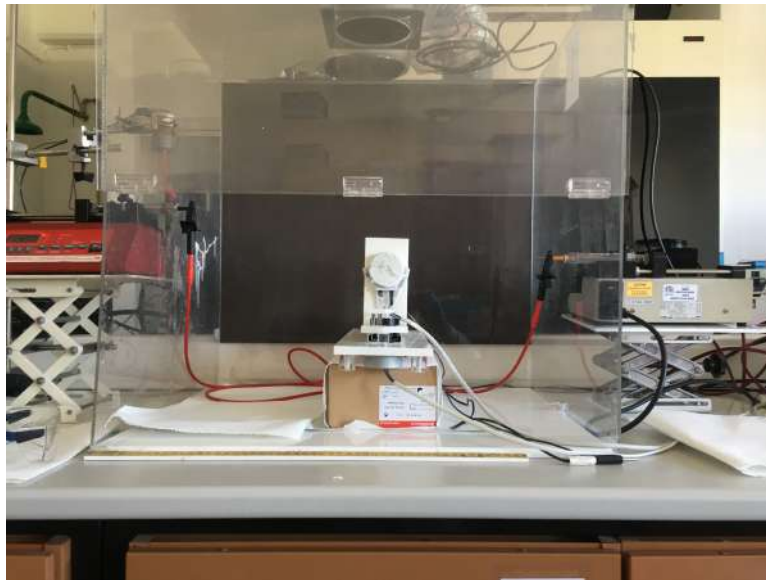


Figure 3.16: Profile picture of the experimental arrangement, where we can see the PEO needle (left) raised 10 cm in relation to the collector.

After about one hour of electro-spinning, there was again a decrease in the crystals in the deposition. This was due to the setting of the sugar crystals in the (inner) base of the syringe. This point was solved by placing a magnet inside the syringe. With a

3.1. DETERMINATION OF THE SCAFFOLDS PRODUCTION PARAMETERS

magnetic stirrer, close to the syringe, it is possible to keep the stirred solution inside the syringe throughout the entire deposition (Figure 3.17). This way we have a constant flow of porogenic agent throughout the entire electrospinning process.



Figure 3.17: Seringe with the PEO solution with the porogenic agent inside and a magnet.

When dissecting a PEO/G# sample, we can observe that the crystals preserve their shape and size. Thus, the efficacy of chloroform saturation with sucrose can be confirmed to avoid dissolution of the porogen, as shown in the following figures, with the size G4 sugar crystals as an example (Figure 3.18 and 3.19).

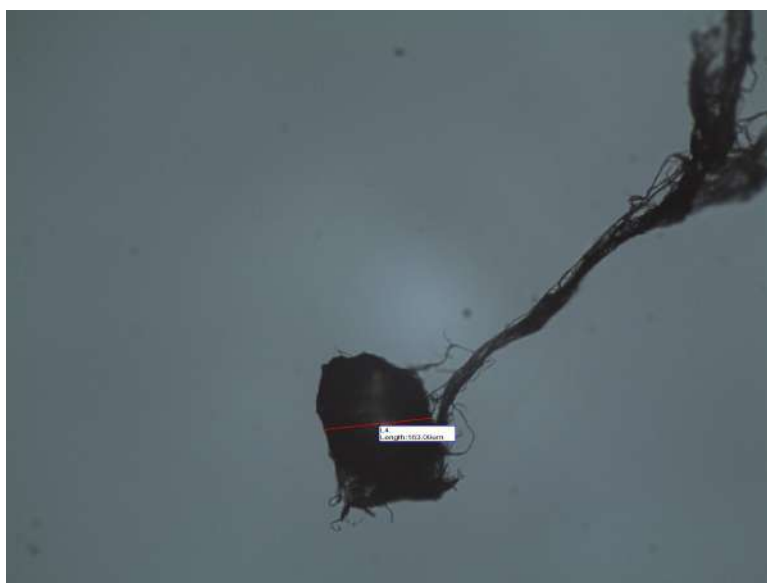


Figure 3.18: G4 dissected crystal from a scaffold with the right size.

It is also possible to verify that the morphology of the fibers did not undergo any



Figure 3.19: Another G4 dissected crystal with similar size.

significant alteration by the presence of the sugar crystals, as it can be seen on Figure 3.20.

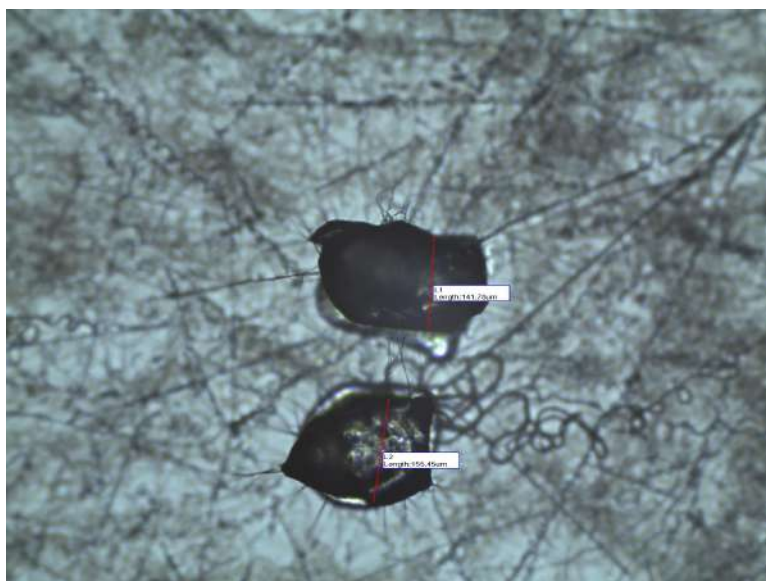


Figure 3.20: PEO fibers with two G4 crystals electrospun on a glass slide.

PCL: GEL + PEO/G# scaffold electrospinning

For the production of the hybrid matrices, it was possible to combine the studied parameters individually for each of the fibers used (PCL:GEL and PEO/G#). The syringes placed on opposite sides of the collector, and the 16kV voltage that had already been fixed for both solutions. It was decided to turn off the electric motor that controls the perpendicular translation movement of the collector because it was in phase with the

rotation motor, making the deposition, not uniform but spiraling along the cylinder. Only the rotation movement in the cylindrical manifold, fixed at 3.75 rpm (revolutions per minute), was used.

3.2 Scaffolds Characterization

3.2.1 Morphology

3.2.1.1 After Electrospinning

In Figure 3.21, we can see the PCL:GEL matrix after electrospinning. It is possible to observe a good fiber morphology. There is no presence of clusters or beads. The fibers are all similar, and also appear to be structurally similar to a native ECM.

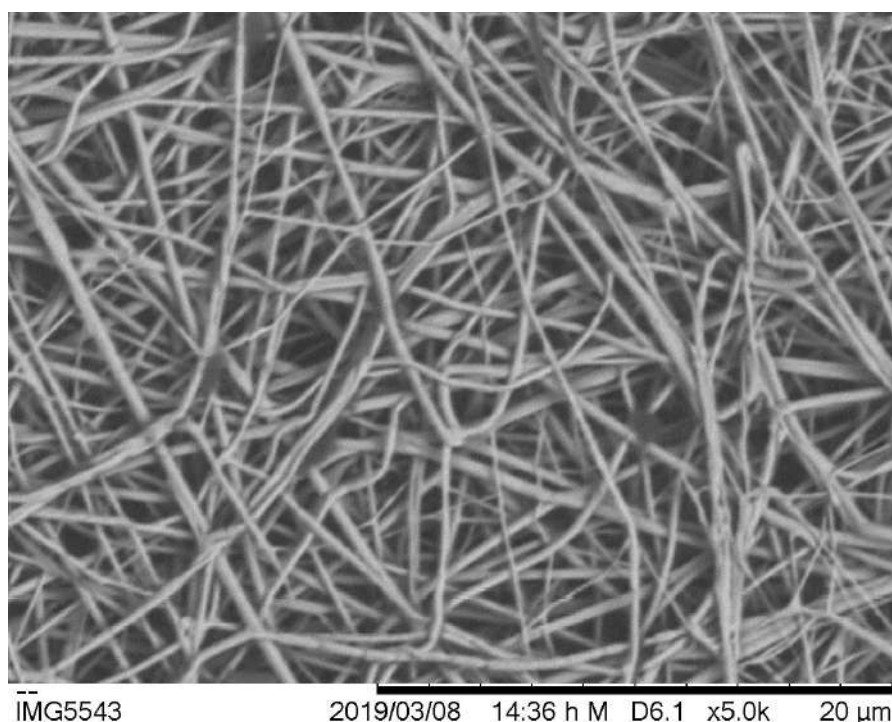


Figure 3.21: PCL:GEL matrix after electrospinning.

The diameters observed in this deposition are all of the same order of magnitude and have an average diameter of (250nm). The measured mean diameter is in agreement with the literature, and therefore we can guarantee that both the solution and the electrospinning parameters used are correct.

In Figure 3.23 and Figure 3.24, we can observe PEO depositions with two different dimensions of sugar crystals - 50 μm to 100 μm and 150 μm to 200 μm , respectively. We can, therefore, confirm that the grains do not lose significant mass during deposition. It is possible to observe that they retain their shape and that no dissolution of the sugar is

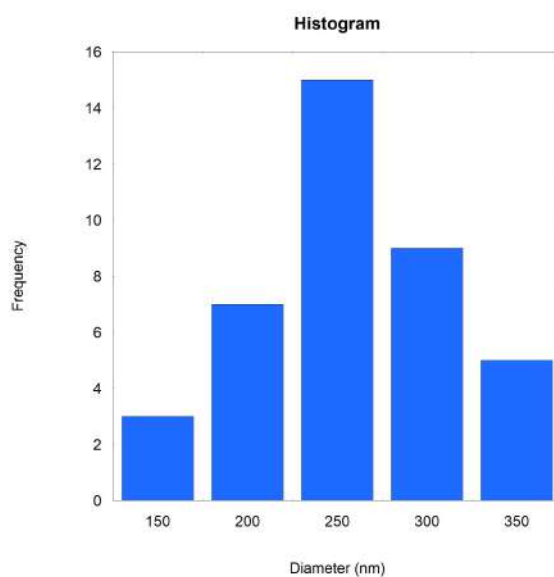


Figure 3.22: PCL:GEL

observable. Due to this, we can conclude that the saturation of the chloroform solvent with sucrose during the production of the solutions prior to the addition of the porogenic agent, has proved to be effective in preventing the dissolution of the sugar crystals.

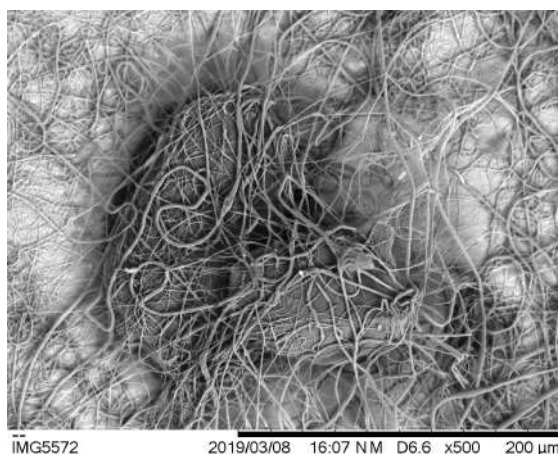


Figure 3.23: PEO fibers around G2 crystals.

PEO fibers also appear to have a good morphology to be used as sacrificial fibers, and although the diameters of the PEO fibers are not uniform, there is no presence of solution agglomerates or beads. These PEO depositions reveal that both PEO solutions and electrospinning parameters are correct for this experimental work.

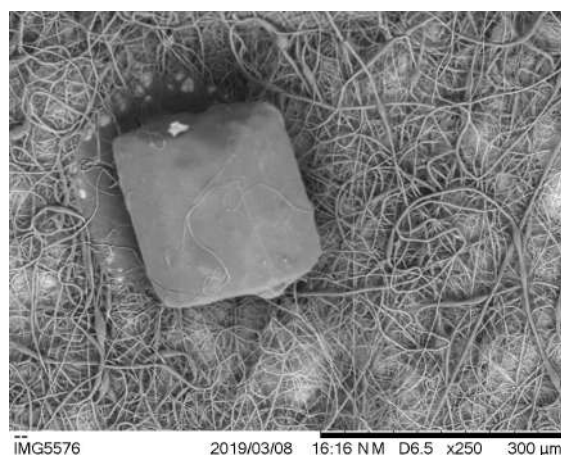


Figure 3.24: PEO fibers around G4 crystals.

3.2.1.2 After Crosslinking

In order to evaluate the structural changes caused by this process to the matrices, SEM images were taken of the matrices after crosslinking.

Figure 3.25 and Figure 3.26 respectively represent the PCL:GEL fibers, crosslinked for 4h and for 1h. Comparing them, we can verify that there is no significant change in the morphology nor in the diameters of the fibers. The crosslinking process has no appreciable structural impact on electrospun PCL:GEL fibers.

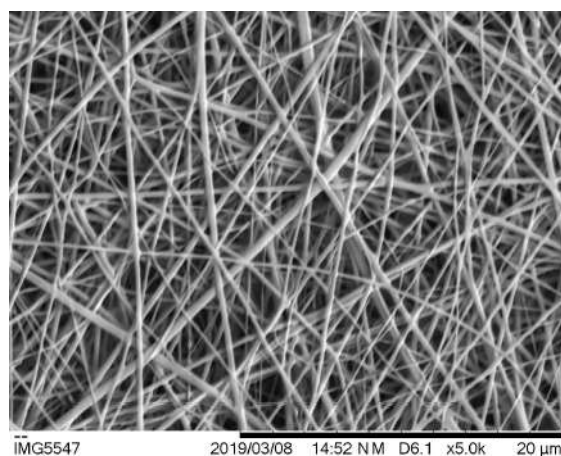


Figure 3.25: PEO fibers around G2 crystals.

In Figures 3.27, 3.28; and 3.29, we can see the PCL:GEL + PEO matrices, already with the addition of the grains of sugar and crosslinked. A slight dissolution of the PEO fibers and the sugar grains is observable. This can be explained by the release of water vapor from the GTA solution during the crosslinking treatment. This slight dissolution is not worrisome, because both PEO fibers and sugar grains are removed in the next stage of washing, and in general no significant changes are observed in the fibers, and it is still

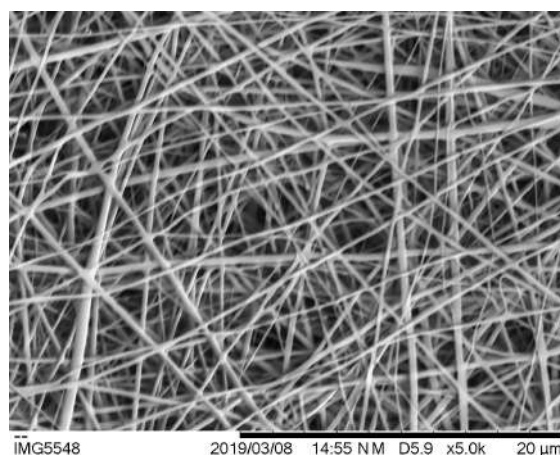


Figure 3.26: PEO fibers around G4 crystals.

possible to observe the matrix composed of micro and nano-fibers.

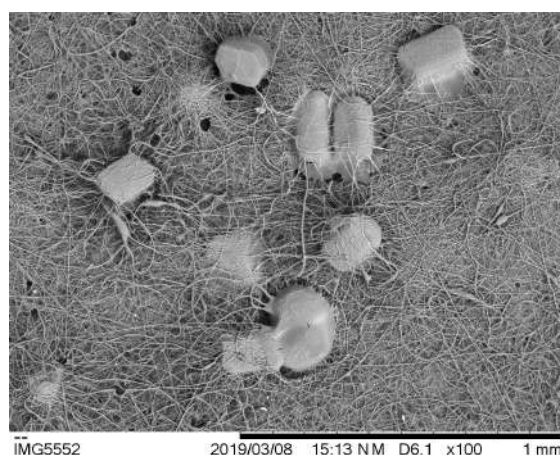


Figure 3.27: PCL:GEL + PEO/G4 (x100 magnification)

3.2.1.3 After Washing

In Figures(3.30, 3.31, 3.32, and 3.33), we can observe the crosslinked and non-crosslinked PCL:GEL fibers after they have been washed. This washing served to simulate what would happen to the PCL:GEL fibers during the removal of the sacrificial fibers and the porogenic agent. It can be observed that non-crosslinked matrices do not preserve their structure or diameters. It is also possible to verify that the matrices lose porosity because, upon the dissolution of uncrosslinked gelatin, the spaces that were previously empty between the fibers are now filled with polymer. The fibers were melted together. This demonstrates that if non-crosslinked matrices were used, there would probably be no benefit from the subsequent removal of the PEO fibers nor the sugar crystals since the matrices would become too dense.

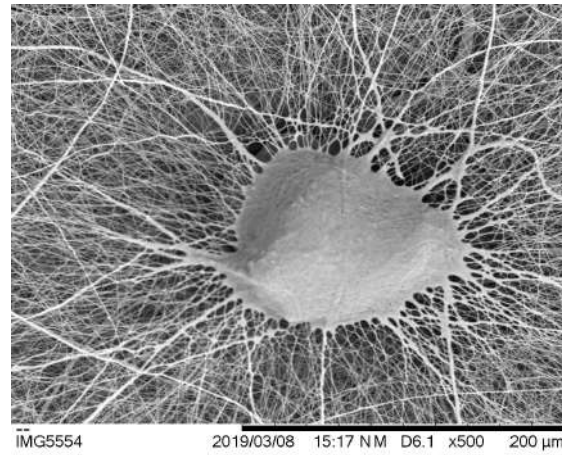


Figure 3.28: PCL:GEL + PEO/G4 (x500 magnification)

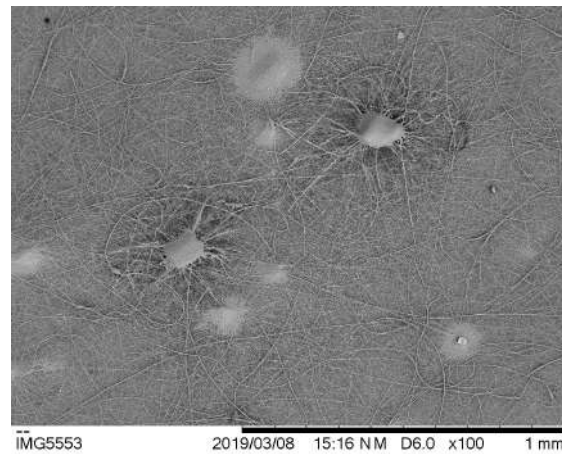


Figure 3.29: PCL:GEL + PEO/G4 (x100 magnification)

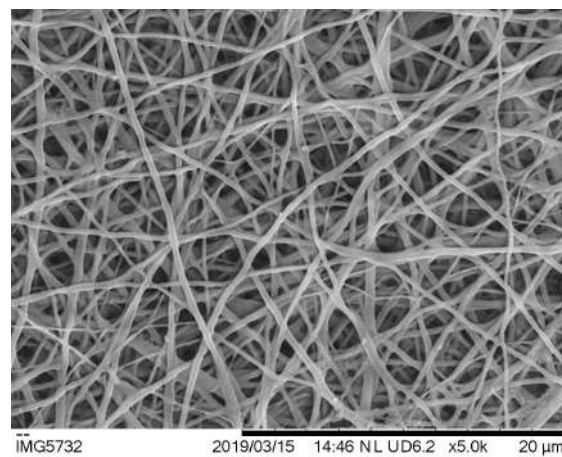


Figure 3.30: PCL:GEL + PCL:GEL + PEO/G4 (x5000 magnification), after washing and crosslinked

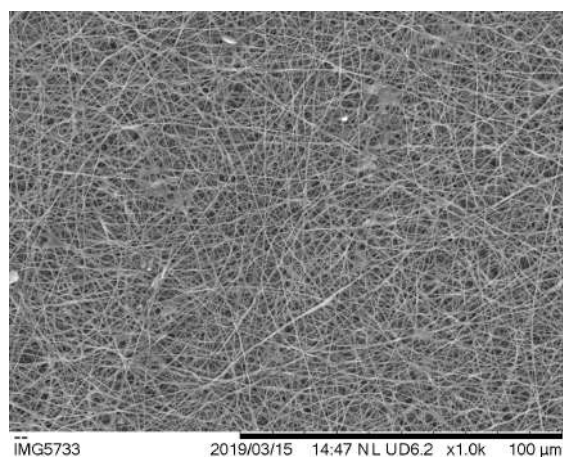


Figure 3.31: PCL:GEL + PCL:GEL + PEO/G4 (x1000 magnification), after washing and crosslinked

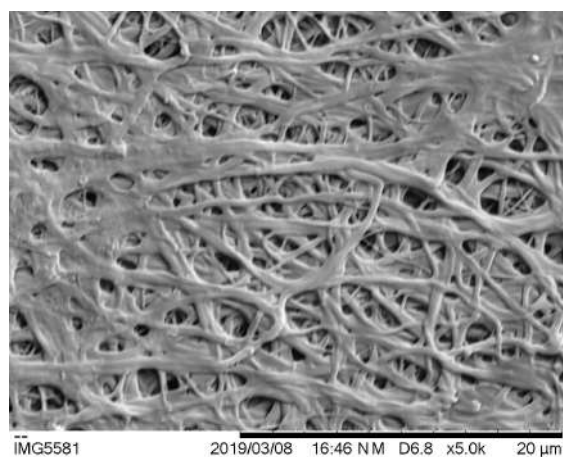


Figure 3.32: PCL:GEL + PCL:GEL + PEO/G4 (x5000 magnification), after washing and not crosslinked

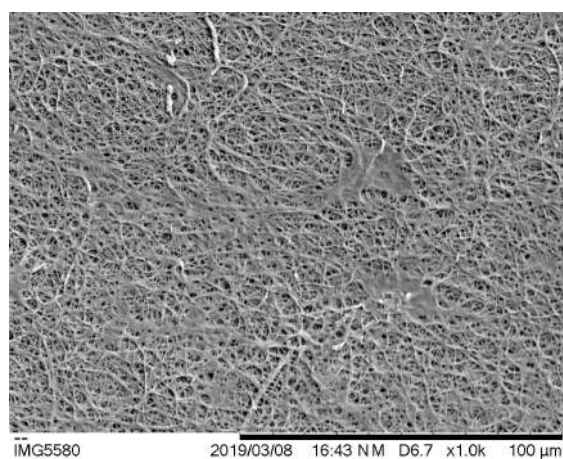


Figure 3.33: PCL:GEL + PCL:GEL + PEO/G4 (x1000 magnification), after washing and not crosslinked

We can see the final appearance of the crosslinked matrices after removal of PEO and sugar crystals in Figure 3.34. It is not possible to assess accurately about the effective increase of matrix porosity, but there seems to be good interconnectivity between the spaces within the substitute. Moreover, after confirming the good deposition and correct interweaving of the PCL:GEL fibers with the PEO fibers, we can affirm that at least the PEO fibers prevented a greater number of connections that could possibly exist between the PCL:GEL fibers. The lower number of connections may not explicitly increase the porosity of the matrices produced but may facilitate the relocation of the fibers by the cells, enhancing cellular infiltration in the substitute.

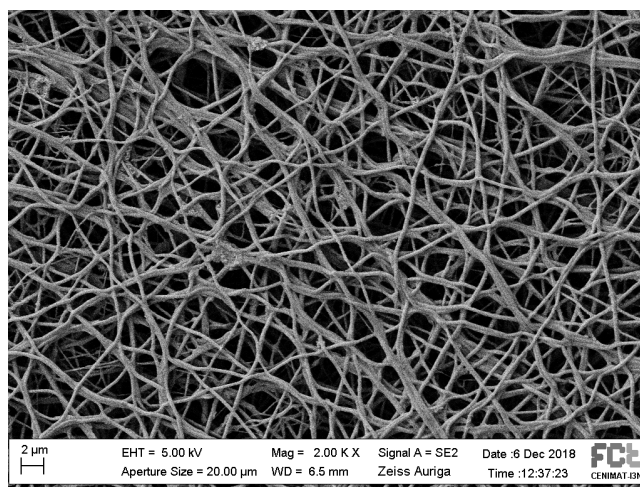


Figure 3.34: PCL:GEL + PCL:GEL + PEO/G4 (x6000 magnification), after washing and crosslinked

The fibers appear to have maintained the ECM-like appearance. It is a good indication that the technique used for washing the sacrificial fibers and the porogenic agent can be safely used without damaging the PCL:GEL fibers we want to preserve. We may also observe small residues of PEO or sugar, however, they are in very reduced quantities and should disappear when using the matrices in physiological applications or in vitro tests, where the aqueous medium will dilute the remaining residues.

3.2.2 Mass Loss Assays

Mass loss tests were performed on the PCL:GEL matrices treated with different crosslinking times - 0h, 1h, 2h, 3h and 4h.

As we can see in the graph of the previous figure, the mass loss is smaller, for greater times of crosslinking as expected.

The cross-linking of gelatin by GTA vapors is effective in creating new bonds between the gelatin proteins, which reduces their degradation when in an aqueous medium. We can verify that the mass loss for the non-crosslinked PCL:GEL matrix is about 50%, which is in agreement with the relative amount of gelatin in the solution - a one-to-one relationship with PCL.

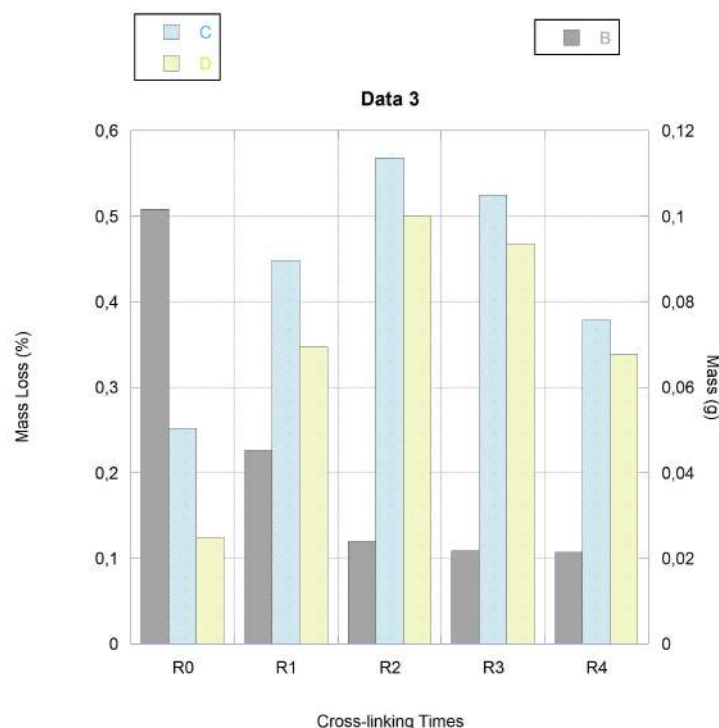


Figure 3.35: PCL:GEL mass loss for the different crosslinking times. Where B is mass loss in percentage, (C) is the initial mass, and (D) is the final mass.

After two hours of crosslinking the mass loss stabilizes and it is almost irrelevant to treat the matrices with GTA vapors for more than two hours. However, as seen in the morphological analysis, the treatment with GTA during the 4h did not damage the scaffolds. To ensure that crosslinking is always effective, we have chosen to treat with GTA during these 4 hours (over-tolerance) for the production of all scaffolds.

During the mass loss tests, it was readily apparent that matrices not treated by GTA rapidly lost the characteristic yellow color of gelatin when submerged in water - this is in accordance with the data obtained in this test.

3.2.3 ATR-FTIR

FTIR assays were performed on the PCL:GEL cross-linked samples (for: 1, 2, 3, and 4 hours) and uncrosslinked samples. These tests served to compare the vibration modes obtained in the spectra with those described in the literature [28] and thus to see if the desired reactions are present in the crosslinking process used in this work.

In the following graphs, the four characteristic peaks of gelatin are found in our spectra as described in the literature (Figure 3.36).

- A peak at 1640 cm^{-1} corresponding to Amide I, and that is the (C = O) stretch of gelatin.

- The peak corresponding to Amide II is visible, between 1542 cm^{-1} and 1544 cm^{-1} . This peak is due to the (C-H) stretch plus (N-H) flexion.
- At 1240 cm^{-1} , we have a peak corresponding to Amide III, which is the (C-N) stretch plus the in-phase flexion of the (N-H) bond.
- Finally, a peak at 3300 cm^{-1} can be seen, corresponding to Amide A which is the mode of vibration of the (N-H) stretch.

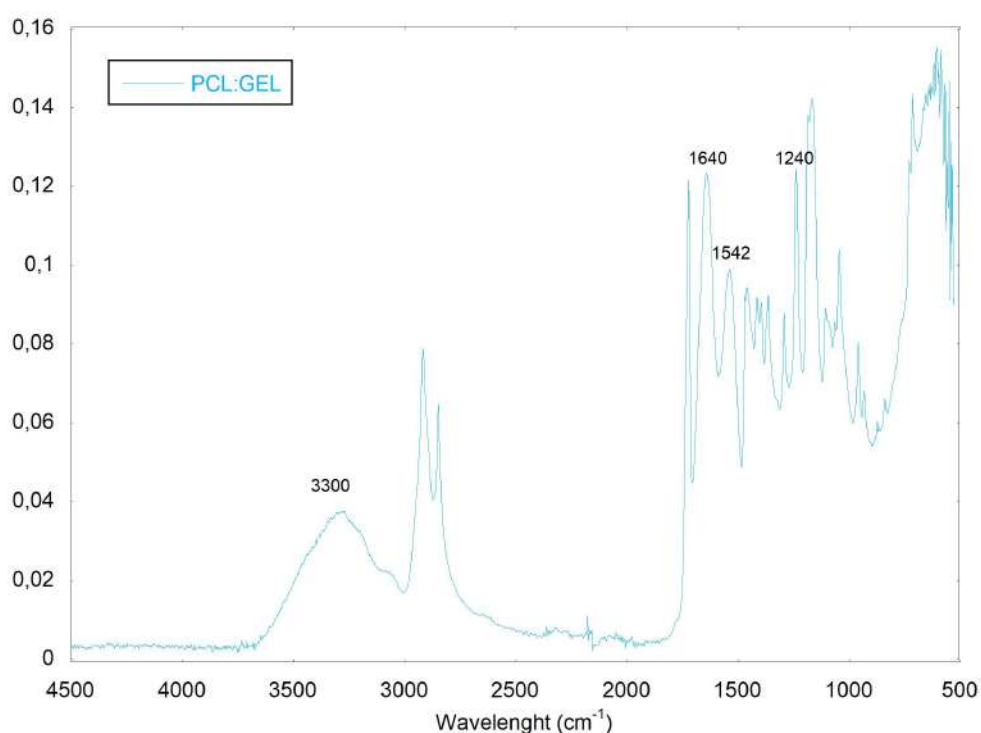


Figure 3.36: PCL:GEL scaffold with the four characteristic peaks of gelatin represented.

Throughout the various crosslinking times (R0, R1, R2, R3 and R4), it can be seen that the ratio of peak 1640 cm^{-1} to peak 1542 cm^{-1} increases with the crosslinking time. This results from the decrease of the peaks corresponding to Amide II, as expected according to the bibliographic description (Figure 3.37).

During crosslinking, it is also possible to observe a substantial color difference between the crosslinked and non-crosslinked matrices. The crosslinked matrices have a characteristic yellowish color of the Aldimine ($\text{CH}=\text{N}$) bonds, which occur due to reactions between the Aldehyde ($-\text{CHO}$) groups of the GTA and the Lysines group present in the gelatine protein residues.

We can conclude that the main characteristics described in the literature regarding the crosslinking of gelatin by GTA were observed.

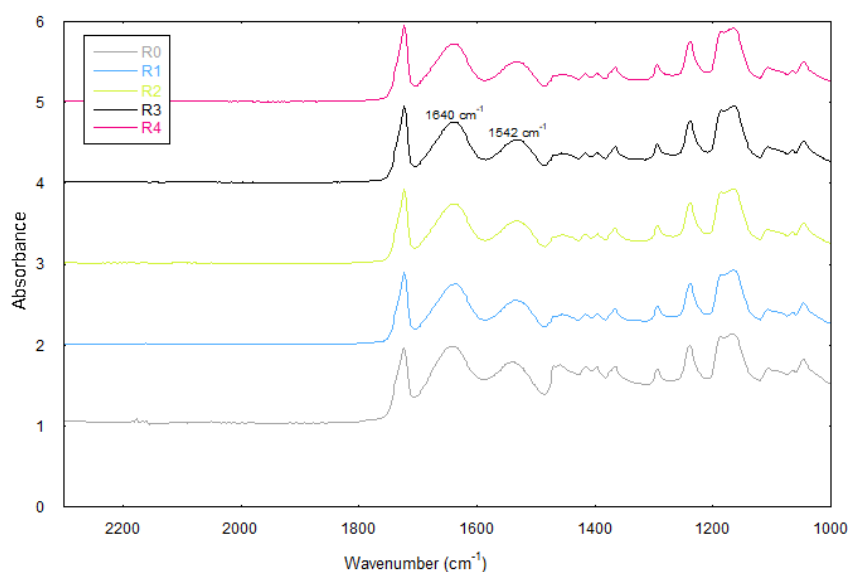


Figure 3.37: ATR-FTIR absorbance spectrum for different crosslinking times.

Table 3.1: Amida I and Amida II FTIR intensities absorbance table for the PCL:GEL scaffolds different crosslinking times.

Crosslinking Times	Relative intensity to the following absorbances	
	1640 cm ⁻¹	1542 cm ⁻¹
RO	3810	2754
R1	3762	2688
R2	3730	2655
R3	3631	2516
R4	2459	1912

Table 3.2: The ratio between Amida I and Amida II relative absorbance intensities, for the PCL:GEL scaffolds different crosslinking times.

Crosslinking Times	Absorbances intensities ratio
	1640 cm ⁻¹ /1542 cm ⁻¹
RO	1,286
R1	1,366
R2	1,405
R3	1,417
R4	1,443

3.2.4 Fluorescence Assays

Through the fluorescence staining, we were able to distinguish the fibers that make up the final matrices. We can thus confirm good deposition and entanglement. By washing the Microscope slide where the deposition was made, we can also confirm the efficacy of water in removing the sacrificial fibers.

Droplets of the PCL solution were made with rhodamine B and PEO with fluorescein, directly on slides. This allows, by comparison, to perceive and predict how the fibers are visible in the fluorescence assay and to recognize which fibers we are observing.

- The PCL doped with rhodamine B, when irradiated at the different wavelengths available in the epifluorescence microscope, was visible as follows: intense orange when irradiated with green light (Figure 3.38); light green when irradiated with blue light. When irradiated with UV light, rhodamine is not fluorescent.



Figure 3.38: PCL with Rhodamine B irradiated with green light.

- The fluorescein doped PEO was visible with the following characteristics: red when irradiated with green light; intense green when irradiated with blue light (Figure 3.39)

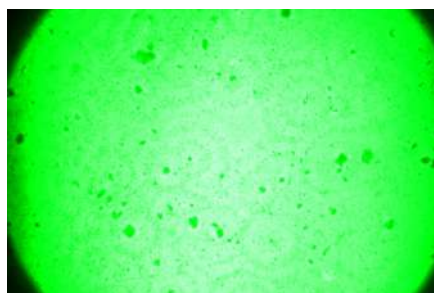


Figure 3.39: PEO with Fluorescein irradiated with blue light.

In the following figures, we can see the deposition of PCL + PEO fibers. The good distribution of both PCL and PEO fibers is observable. By fluorescence assay, they are easily distinguishable, which is not possible when using bright field nor phase contrast microscopy (Figure 3.40).

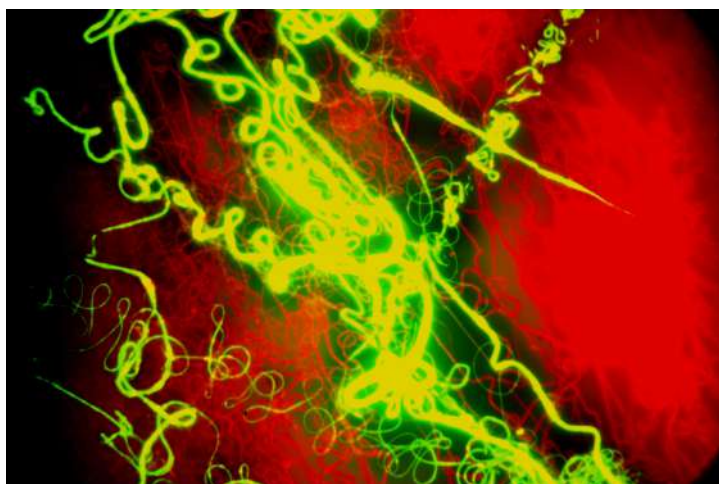


Figure 3.40: PCL and PEO fibers deposition. The PCL fibers in orange and the PEO fibers in green are clearly visible in this image.

During the washing process, the PCL fibers were contaminated by the fluorescein dye that was present in the PEO sacrificial fibers which were dissolved, therefore, they became also reactive to the same wavelengths to which the PEO fibers were. However, as we can see in the figures, by superimposing the images we can verify that all fibers represented in red overlap the fibers represented in green, which reveals the presence of a single type of fibers in the glass slides. In such figures, it is also possible to compare the deposition before and after washing and to realize that there is a substantial reduction in the density of fibers present (Figure 3.41).

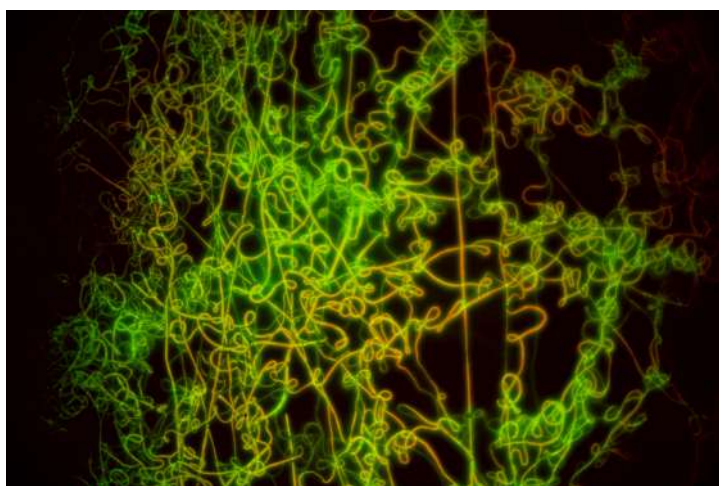


Figure 3.41: In this image is clearly visible that only PCL fibers are present. It is also noticeable the yellowish color present on the fibers due to PCL contamination with fluoresceins residues during PEO dissolution.

We conclude therefore that the removal of the sacrificial fibers made with water, and following the experimental procedures used in this work, is effective.

3.2.5 Tensile Tests

The concern with the mechanical properties of the matrices developed in this work results from the possible weakening from the washing process or from making them more brittle through the crosslinking process. During the process of removal of the sacrificial fibers and the porogenic agent, there may be a general weakening of some mechanical properties of the matrices. The matrices are expected to increase their ability to promote cell infiltration, but it must be borne in mind that these substitutes have to be designed so that they can be used in living beings in the future and handled by a surgeon with some ease in order to be able to be implanted. Developing something that allows a good cellular infiltration, but not provides sufficient support for the tissues that we want to regenerate is not desirable.

The assays were made to the matrices produced, cross-linked with GTA during 4h and after washing for removal of the sacrificial fibers and porogenic agent.

It was planned to make the tests with the dry matrices, to be easier to compare with other works already done in GREAT. However, it is quite difficult to remove the dry matrices from the aluminium foil. When dried some matrices, especially those that previously had PEO in their composition become too brittle and wind up on themselves. In this way, it is impossible to secure the uniform traction of the matrices and collect data about its dimensions precisely (Figure 3.42).



Figure 3.42: The aspect of dry samples.

It was decided to make the mechanical tests with the wet samples. The data collected from the tensile tests with the wet samples are also more realistic since these matrices are for use in a wet physiological medium. With the wet matrices, it was possible to make the tensile tests, however, the matrices were prone to cutting and often the clamps of the tensile equipment were enough to invalidate the test by making small cuts in the samples.

From the tensile tests performed on each of the six matrices produced, data about Young's modulus, fracture stress, and percent deformation were obtained and can be seen in the following figure.

Table 3.3: Tensile tests data results.

Scaffold	Young's Modulus (MPa)	UTS (MPa)	Strain (%)
PCL:GEL	$5,1 \pm 0,5$	$1,9 \pm 0,2$	12 ± 2
PCL:GEL+PEO/G0	$3,8 \pm 0,7$	$1,8 \pm 0,2$	25 ± 2
PCL:GEL+PEO/G1	$3,4 \pm 0,4$	$2,0 \pm 0,2$	26 ± 3
PCL:GEL+PEO/G2	$3,7 \pm 0,7$	$2,3 \pm 0,4$	16 ± 2
PCL:GEL+PEO/G3	$4,4 \pm 0,7$	$3,1 \pm 0,2$	14 ± 1
PCL:GEL+PEO/G4	$4,0 \pm 0,3$	$1,2 \pm 0,2$	11 ± 3

Based on the values obtained, we can observe a difference of 1 MPa in the Young's Modulus between the PCL:GEL matrix and the PEO/G0, G1 and G2 matrices. In the case of the larger crystals, we already have almost equal values of deformation and Young's modulus. One reason for this may be in the presence of the crystals. Because the amount of grain to be added in the solution has been made in percentage by weight, it means that for smaller crystals we will have more crystals in solution. The matrices with smaller crystals will have the porogenic agents/sacrificial fibers much more uniformly distributed on their surface and with that its presence in mechanical tests is more detectable. If we remember SEM images, we can also see that the larger grains carry with them large amounts of PEO, leaving the PCL:GEL fibers around them with low distribution. This can also be a valid hypothesis for these differences.

However, these variations are not significant, and possibly, if more mechanical tests were done on all matrices, the results would tend to be closer.

Knowing that the Young's Modulus represents the rigidity of a material, in comparison with Young's Moduli of other biological tissues and substitutes for tissue engineering, we can say that these matrices have excellent mechanical properties.

According to the literature, the stiffness of the porcine carotid arteries is on the order of 13 MPa (native) and 20 MPa when decellularized - the ECM of these tissues. In the obtained data, we can see that the higher Young's Modulus we have, is nonetheless, inferior to the natural decellularized ECM matrix. Also in the literature, we can observe stiffness data for PCL:GEL matrices (1:1) with identical values - varying between 2 MPa and 3 MPa. As the objective of this work is the development of a matrix that approaches the native ECM, obtaining a deposition with greater tensile strength than the original is relevant data.

The stress at which rupture happens, although lower than that of the native ECM (about 2.5 MPa) and also that the decellularized (about 4.3 MPa), is not significantly lower and is of the same order of magnitude.

In fact, during the procedures, it was remarkable how easily these samples when wet were handled, without great risk of damaging them. In spite of their small thickness, they

always returned to their original shape.

3.3 *In Vitro* Assays

Seeding was performed on the different matrices produced (PCL:GEL and PCL:GEL + PEO/G#), to measure and quantify the scaffolds capacity to provide cell adhesion and proliferation - cell viability.

3.3.1 Adhesion and Proliferation

To assess the adhesion capacity of the cells to the matrix, a cell viability assay was performed with resazurin at around 24h of seeding. Through the analysis of the following graph [3.44](#), we can conclude that all the different matrices promote good and rapid cell adhesion. This is in accordance with the ability of gelatin to promote cell adhesion and its presence in all matrices used.

In order to assess cell proliferation, cell viability assays were performed with resazurin every 3 days, up to 12 days of cell culture. In the following graph [3.44](#), we can recognize that although cell adhesion is substantially greater in the adherent culture plate control wells, cell proliferation in the matrices or wells is similar. It is quantifiable that relative cell proliferation in all substitutes is approximately the double after 12 days of culture.

It is possible to conclude that the solutions used and the matrices developed have the potential to give good substitutes in tissue engineering and that if the structural properties, such as porosity, pore size, and interconnectivity are present, these matrices have a great possibility of promoting cell infiltration.

3.3.2 Cell Infiltration

After 12 days of seeding, the cells were fixed in the samples with paraformaldehyde and then stained with DAPI. It is thus possible through the visualization of the cellular nuclei, to observe the presence of the cells on the surface of the samples. If cells are visible on the opposite side of the matrices to the face where the seeding was performed, we can conclude that the cells would have migrated along the total thickness of the deposition.

In the following figures [3.45](#) it is possible to observe the presence of cells on the surface of the samples.

On the opposite faces of the matrices it was not possible to detect any cell present. This does not mean that there has been no cell infiltration. Cell infiltration in the interior, is possibly much slower than proliferation on the scaffold surface. It is also possible that there were cells migrating inside the matrices, but that have not yet had time to travel the entire distance between one side and the other of the matrix. The surface of the matrices because it is not yet confluent is a good indication that the cells have a slow proliferation, in addition to that, the HFFF2 are considerably large cells. We can infer that there is cell proliferation on the surface of the matrices and that it would be good to evaluate further

cultures for a longer period. With a confluence of about 80-90% on the surfaces of the samples, the cells would be more likely to migrate into the scaffold where there is greater resistance to cell migration than on the surface.

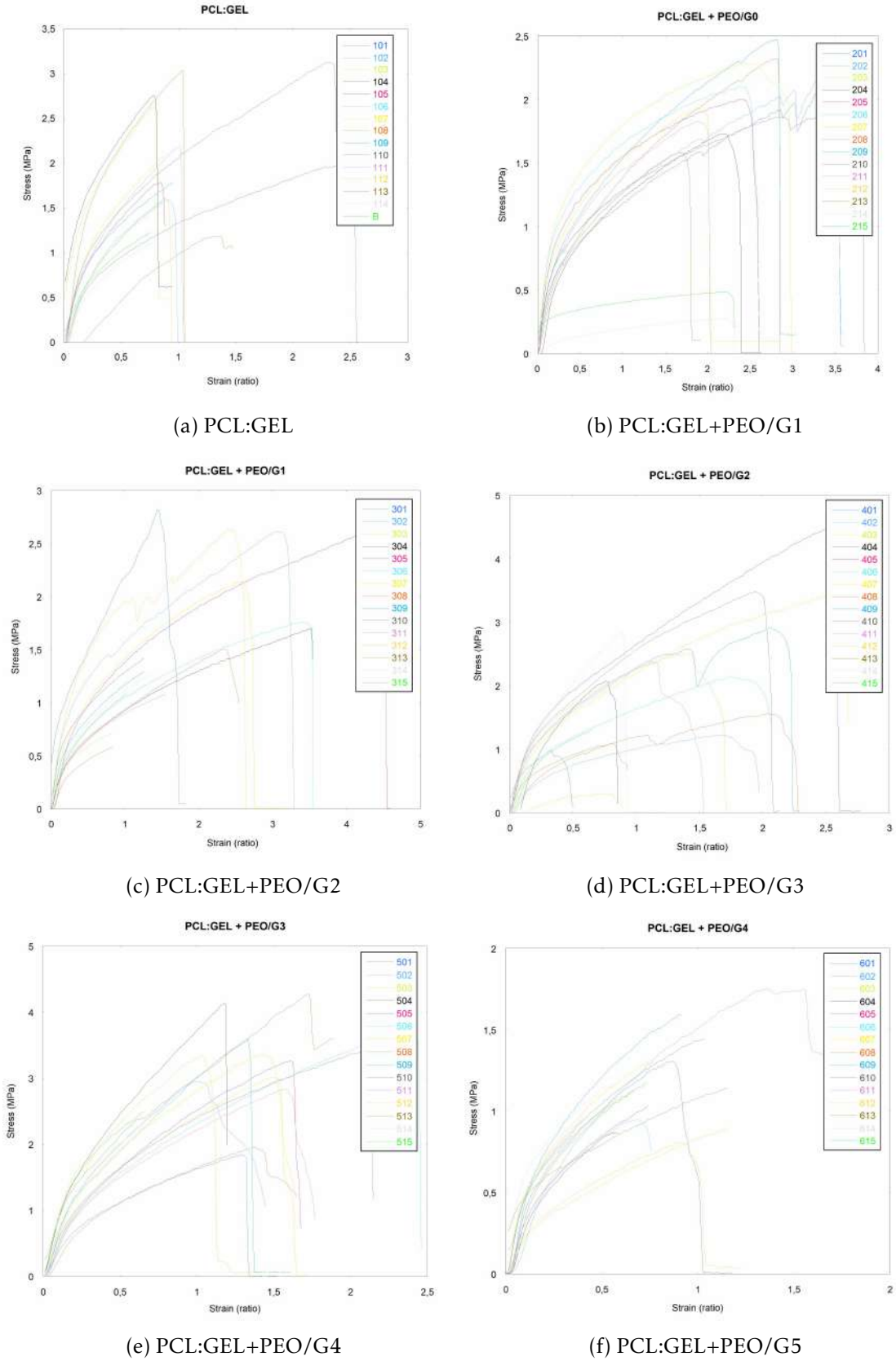


Figure 3.43: Stress-Strain curve graphs.

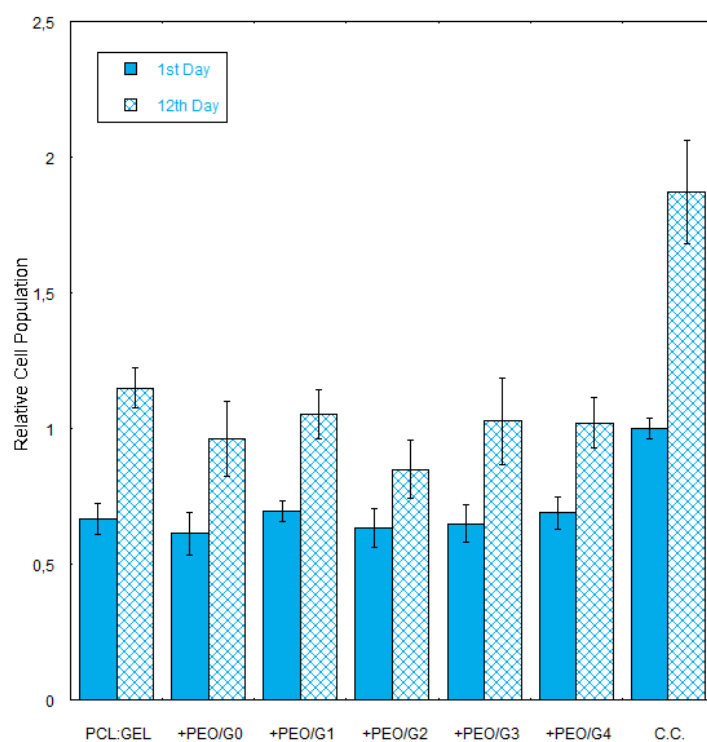


Figure 3.44: The 24 hours and 12 days cell culture viability assay of the six different scaffolds.



Figure 3.45: DAPI assay of the 12 days cell culture with the general cells distribution on the surface of the samples.

CONCLUSIONS AND FUTURE PERSPECTIVES

The aim of the present dissertation was to study the combination of two techniques previously described in the literature, to increase porosity, pore size, and interconnectivity in 3D matrices produced by electrospinning. The two techniques chosen were the use of sacrificial fibers and a porogenic agent.

In the production of the solutions, PEO was chosen for the production of the sacrificial fibers and sucrose (pastry sugar crystals) was chosen as the porogenic agent. This choice of materials results from both being readily water soluble and the purpose of increasing pore size for potentiating cellular migration to the matrices' interior. Both the PEO and sucrose were used with PCL and gelatin that constitute the primary fibers and are biocompatible and biodegradable.

The optimization of the production parameters by electrospinning of six different matrices was achieved. A conventional matrix in co-deposition of PCL:GEL, a hybrid matrix composed of PCL:GEL with PEO fibers, and four other matrices composed of PCL:GEL with PEO fibers with four different grain sizes. The choice of four different grain sizes, used in the solution always in the same percentage, served to understand how different grain sizes may interfere with the structure of substitutes or cell infiltration.

To evaluate the crosslinking of the matrices, mass loss, SEM and FTIR analysis was performed. It was found that two hours of crosslinking were sufficiently effective, however, since the matrices would subsequently be washed, it was decided to crosslink for 4 hours, and thus ensure the effectiveness of the treatment. The matrix washing process was done by submerging the matrices in a glycine solution. Glycine reacts with any GTA residue which may still be present from the crosslinking process.

During the morphological analysis of the matrices produced it was found that the PCL:GEL matrices are in agreement with previous work, and that the washing and

crosslinking processes do not lead to the appearance of significant defects in the substitutes. There was no record of the appearance of agglomerates, beads, or broken fibers in the electrospun matrices. In addition, after washing, although small deposits of PEO and sugar are visible, the primary fibers (PCL:GEL) look good and are not fused together - this may be significant for an increase in porosity in the matrices.

The morphology of PEO fibers and sugar grains looks equally good. The fibers are well distributed and have diameters slightly higher than the primary fibers. The sugar grains after electrospinning preserve their shape and size, which shows that the pre-saturation of the chloroform solvent with sucrose for the production of the solutions is sufficient to prevent the dissolution of the porogenic agent before the deposition of the fibers.

We can also observe a homogenous distribution of the porogenic agent - represents that the parameters chosen for the good electrospinning of the PEO fibers are equally good for the fibers while serving as carriers for the sugar grains.

To determine the mechanical characteristics of the matrices, tensile tests were carried out on samples of the different matrices produced. Because the matrices were to be used immersed in physiological medium in the *in vitro* assays, hydrated samples were used for comparison with biological tissues. Mechanical assays revealed mechanical behavior similar to some biological tissues, and the data collected indicate that there would be no impairment due to potential scaffold fragility for use in *in vivo* assays. There were also no significant mechanical differences in the different scaffolds produced - matrices with sacrificial fibers and porogenic agent in the proportion of 1:1 with PCL:GEL fibers were not found to be considerably more fragile matrices after being submerged for fiber and porogen removal.

Fluorescence assays revealed good deposition and entanglement between primary fibers (PCL) and sacrificial fibers (PEO). They also confirmed the efficient removal of the sacrificial fibers through the protocol defined for the submersion of the matrices in water.

In vitro assays have shown that the matrices produced are scaffolds which provide a surface with good cell adhesion. We also conclude that although initial cell adhesion is not as efficient as in control wells, proliferation throughout the culture is already very similar and efficient.

At 12 day seeding, it was not possible to draw final conclusions about cell infiltration. The cells used (HFFF2) are large (even when elongated) and as long as there is no confluence of approximately 80-90% at the surface of the samples the cells should not move inward where there is greater resistance to their displacement.

For future work, it is suggested to make *in vitro* tests with a longer duration, ensuring that there is cell confluence on the surface of the samples when fixing the samples to evaluate cellular infiltration.

It would also be relevant to study different amounts of porogenic agent and sacrificial fibers in the matrices. The following changes are suggested:

- Increase and study of different concentrations of the porogen agent.

-
- Increase and study of different concentrations of PEO in the production of solutions of sacrificial fibers.
 - Increase the flow rate for the PEO solution (with optimized production parameters for the fibers to remain uniform and replicable).

With these adjustments, it may be possible to obtain matrices with greater capacity of cellular infiltration, and at the same time maintain the mechanical and cellular viability characteristics demonstrated in this dissertation.

BIBLIOGRAPHY

- [1] J. M. Anderson, A. Rodriguez, and D. T. Chang. "Foreign body reaction to biomaterials." In: *Seminars in Immunology* 20.2 (2008), pp. 86–100. ISSN: 10445323. DOI: [10.1016/j.smim.2007.11.004](https://doi.org/10.1016/j.smim.2007.11.004).
- [2] B. Azimi, P. Nourpanah, M. Rabiee, and S. Arbab. "Poly (lactide -co- glycolide) Fiber : An Overview." In: *Journal of Engineered Fibers and Fabrics* 9.3 (2014), pp. 74–90. ISSN: 15589250. URL: <http://www.jeffjournal.org>.
- [3] S. F. Badylak, D. O. Freytes, and T. W. Gilbert. "Reprint of: Extracellular matrix as a biological scaffold material: Structure and function." In: *Acta Biomaterialia* 23.S (2015), S17–S26. ISSN: 18787568. DOI: [10.1016/j.actbio.2015.07.016](https://doi.org/10.1016/j.actbio.2015.07.016). URL: <http://dx.doi.org/10.1016/j.actbio.2008.09.013>.
- [4] B. M. Baker, A. O. Gee, R. B. Metter, A. S. Nathan, R. A. Marklein, J. A. Burdick, and R. L. Mauck. "The potential to improve cell infiltration in composite fiber-aligned electrospun scaffolds by the selective removal of sacrificial fibers." In: *Biomaterials* 29.15 (2008), pp. 2348–2358. ISSN: 01429612. DOI: [10.1016/j.biomaterials.2008.01.032](https://doi.org/10.1016/j.biomaterials.2008.01.032). arXiv: NIHMS150003.
- [5] N. Bhardwaj and S. C. Kundu. "Electrospinning: A fascinating fiber fabrication technique." In: *Biotechnology Advances* 28.3 (2010), pp. 325–347. ISSN: 07349750. DOI: [10.1016/j.biotechadv.2010.01.004](https://doi.org/10.1016/j.biotechadv.2010.01.004).
- [6] R Chandra and R. Rustgi. "Pergamon BIODEGRADABLE POLYMERS." In: *Progress in Polymer Science* 23.97 (1998), pp. 1273–1335. ISSN: 00796700. DOI: [10.1016/S0079-6700\(97\)00039-7](https://doi.org/10.1016/S0079-6700(97)00039-7).
- [7] A. Cipitria, A. Skelton, T. R. Dargaville, P. D. Dalton, and D. W. Hutmacher. "Design, fabrication and characterization of PCL electrospun scaffolds—a review." In: *Journal of Materials Chemistry* 21.26 (2011), p. 9419. ISSN: 0959-9428. DOI: [10.1039/c0jm04502k](https://doi.org/10.1039/c0jm04502k). URL: <http://xlink.rsc.org/?DOI=c0jm04502k>.
- [8] R. Dorati, C. Colonna, I. Genta, T. Modena, and B. Conti. "Effect of porogen on the physico-chemical properties and degradation performance of PLGA scaffolds." In: *Polymer Degradation and Stability* 95.4 (2010), pp. 694–701. ISSN: 01413910. DOI: [10.1016/j.polymdegradstab.2009.11.039](https://doi.org/10.1016/j.polymdegradstab.2009.11.039). URL: <http://dx.doi.org/10.1016/j.polymdegradstab.2009.11.039>.

- [9] J. Doshi and D. H. Reneker. "ELSEVIER Journal of Electrostatics 35 (1995) 151o160 Electrospinning Process and Applications of Electrospun Fibers." In: 35 (1995), pp. 151–160. URL: https://ac.els-cdn.com/0304388695000418/1-s2.0-0304388695000418-main.pdf?{_}tid=c1682b39-d0f2-47f7-8f11-fb5e19c6e3e8{\&}acdnat=1549317377{_}ed3a31030539d445f9191bfb62a8364a.
- [10] L. Ghasemi-Mobarakeh, M. P. Prabhakaran, M. Morshed, M. H. Nasr-Esfahani, and S. Ramakrishna. "Electrospun poly(ϵ -caprolactone)/gelatin nanofibrous scaffolds for nerve tissue engineering." In: *Biomaterials* 29.34 (2008), pp. 4532–4539. ISSN: 01429612. DOI: [10.1016/j.biomaterials.2008.08.007](https://doi.org/10.1016/j.biomaterials.2008.08.007).
- [11] A. Greiner and J. H. Wendorff. "Electrospinning: A fascinating method for the preparation of ultrathin fibers." In: *Angewandte Chemie - International Edition* 46.30 (2007), pp. 5670–5703. ISSN: 14337851. DOI: [10.1002/anie.200604646](https://doi.org/10.1002/anie.200604646).
- [12] Q. Hou, D. W. Grijpma, and J. Feijen. "Porous polymeric structures for tissue engineering prepared by a coagulation, compression moulding and salt leaching technique." In: *Biomaterials* 24.11 (2003), pp. 1937–1947. ISSN: 01429612. DOI: [10.1016/S0142-9612\(02\)00562-8](https://doi.org/10.1016/S0142-9612(02)00562-8).
- [13] Z. M. Huang, Y. Z. Zhang, M. Kotaki, and S. Ramakrishna. "A review on polymer nanofibers by electrospinning and their applications in nanocomposites." In: *Composites Science and Technology* 63.15 (2003), pp. 2223–2253. ISSN: 02663538. DOI: [10.1016/S0266-3538\(03\)00178-7](https://doi.org/10.1016/S0266-3538(03)00178-7).
- [14] D. W. Hutmacher. "Scaffold design and fabrication technologies for engineering tissues–state of the art and future perspectives." In: *Journal of biomaterials science. Polymer edition* 12.1 (2001), pp. 107–24. ISSN: 0920-5063. URL: <http://www.ncbi.nlm.nih.gov/pubmed/11334185>.
- [15] D. W. Hutmacher, T. B. Woodfield, and P. D. Dalton. "Scaffold Design and Fabrication." In: *Tissue Engineering: Second Edition* (2014), pp. 311–346. DOI: [10.1016/B978-0-12-420145-3.00010-9](https://doi.org/10.1016/B978-0-12-420145-3.00010-9). URL: <http://www.sciencedirect.com/science/article/pii/B9780123708694000148>.
- [16] Y. Ikada. "Challenges in tissue engineering." In: *Journal of the Royal Society Interface* 3.10 (2006), pp. 589–601. ISSN: 17425662. DOI: [10.1098/rsif.2006.0124](https://doi.org/10.1098/rsif.2006.0124).
- [17] V. Karageorgiou and D. Kaplan. "Porosity of 3D biomaterial scaffolds and osteogenesis." In: *Biomaterials* 26.27 (2005), pp. 5474–5491. ISSN: 01429612. DOI: [10.1016/j.biomaterials.2005.02.002](https://doi.org/10.1016/j.biomaterials.2005.02.002).
- [18] T. G. Kim, H. J. Chung, and T. G. Park. "Macroporous and nanofibrous hyaluronic acid/collagen hybrid scaffold fabricated by concurrent electrospinning and deposition/leaching of salt particles." In: *Acta Biomaterialia* 4.6 (2008), pp. 1611–1619. ISSN: 17427061. DOI: [10.1016/j.actbio.2008.06.008](https://doi.org/10.1016/j.actbio.2008.06.008).

- [19] Y. Kuboki, H. Takita, D. Kobayashi, E. Tsuruga, M. Inoue, M. Murata, N. Nagai, Y. Dohi, and H. Ohgushi. "BMP-induced osteogenesis on the surface of hydroxyapatite with geometrically feasible and nonfeasible structures: Topology of osteogenesis." In: *Journal of Biomedical Materials Research* 39.2 (1998), pp. 190–199. ISSN: 00219304. DOI: [10 . 1002 / \(SICI \) 1097 - 4636\(199802 \) 39 : 2<190 :: AID - JBM4>3.0.CO;2-K](https://doi.org/10.1002/(SICI)1097-4636(199802)39:2<190::AID-JBM4>3.0.CO;2-K).
- [20] M. Labet and W. Thielemans. "Synthesis of polycaprolactone: A review." In: *Chemical Society Reviews* 38.12 (2009), pp. 3484–3504. ISSN: 03060012. DOI: [10 . 1039 / b820162p](https://doi.org/10.1039/b820162p).
- [21] S. B. Lee, Y. H. Kim, M. S. Chong, S. H. Hong, and Y. M. Lee. "Study of gelatin-containing artificial skin V: Fabrication of gelatin scaffolds using a salt-leaching method." In: *Biomaterials* 26.14 (2005), pp. 1961–1968. ISSN: 01429612. DOI: [10 . 1016 / j . biomaterials . 2004 . 06 . 032](https://doi.org/10.1016/j.biomaterials.2004.06.032).
- [22] M. Li, M. J. Mondrinos, M. R. Gandhi, F. K. Ko, A. S. Weiss, and P. I. Leikes. "Electrospun protein fibers as matrices for tissue engineering." In: *Biomaterials* 26.30 (2005), pp. 5999–6008. ISSN: 01429612. DOI: [10 . 1016 / j . biomaterials . 2005 . 03 . 030](https://doi.org/10.1016/j.biomaterials.2005.03.030).
- [23] W.-J. Li, R. M. Shanti, and R. S. Tuan. *Electrospinning Technology for Nanofibrous Scaffolds in Tissue Engineering*. Vol. 9. 2007. ISBN: 3527313893. DOI: [10 . 1002 / 9783527610419 . nt1s0097](https://doi.org/10.1002/9783527610419.nt1s0097).
- [24] Q. L. Loh and C. Choong. "Three-Dimensional Scaffolds for Tissue Engineering Applications: Role of Porosity and Pore Size." In: *Tissue Engineering Part B: Reviews* 19.6 (2013), pp. 485–502. ISSN: 1937-3368. DOI: [10 . 1089 / ten . teb . 2012 . 0437](https://doi.org/10.1089/ten.teb.2012.0437). URL: <https://www.liebertpub.com/doi/10.1089/ten.teb.2012.0437>.
- [25] J. L. Lowery, N. Datta, and G. C. Rutledge. "Effect of fiber diameter, pore size and seeding method on growth of human dermal fibroblasts in electrospun poly(ϵ -caprolactone) fibrous mats." In: *Biomaterials* 31.3 (2010), pp. 491–504. ISSN: 01429612. DOI: [10 . 1016 / j . biomaterials . 2009 . 09 . 072](https://doi.org/10.1016/j.biomaterials.2009.09.072).
- [26] L. Martinova and D. Lubasova. "Reasons for using polymer blends in the electrospinning process." In: *AIP Conference Proceedings* 1502.1 (2012), pp. 115–128. ISSN: 0094243X. DOI: [10 . 1063 / 1 . 4769138](https://doi.org/10.1063/1.4769138).
- [27] J. Nam, Y. Huang, S. Agarwal, and J. Lannutti. "Improved Cellular Infiltration in Electrospun Fiber via Engineered Porosity." In: *Tissue Engineering* 13.9 (2007), pp. 2249–2257. ISSN: 1076-3279. DOI: [10 . 1089 / ten . 2006 . 0306](https://doi.org/10.1089/ten.2006.0306). arXiv: [15334406](https://arxiv.org/abs/15334406). URL: <http://www.liebertonline.com/doi/abs/10.1089/ten.2006.0306>.
- [28] T.-H. Nguyen and B.-T. Lee. "Fabrication and characterization of cross-linked gelatin electro-spun nano-fibers." In: *Journal of Biomedical Science and Engineering* 03.12 (2011), pp. 1117–1124. ISSN: 1937-6871. DOI: [10 . 4236 / jbise . 2010 . 312145](https://doi.org/10.4236/jbise.2010.312145).

- [29] P. Plikk, S. Målberg, and A. C. Albertsson. "Design of resorbable porous tubular copolyester scaffolds for use in nerve regeneration." In: *Biomacromolecules* 10.5 (2009), pp. 1259–1264. ISSN: 15257797. DOI: [10.1021/bm900093r](https://doi.org/10.1021/bm900093r).
- [30] V. Raeisdasteh Hokmabad, S. Davaran, A. Ramazani, and R. Salehi. "Design and fabrication of porous biodegradable scaffolds: a strategy for tissue engineering." In: *Journal of Biomaterials Science, Polymer Edition* 28.16 (2017), pp. 1797–1825. ISSN: 15685624. DOI: [10.1080/09205063.2017.1354674](https://doi.org/10.1080/09205063.2017.1354674). URL: <http://doi.org/10.1080/09205063.2017.1354674>.
- [31] D. H. Reneker and I. Chun. "Nanometre diameter bres of.pdf." In: 7 (1996), pp. 216–223.
- [32] W. S. Sheridan, G. P. Duffy, and B. P. Murphy. "Mechanical characterization of a customized decellularized scaffold for vascular tissue engineering." In: *Journal of the Mechanical Behavior of Biomedical Materials* 8 (2012), pp. 58–70. ISSN: 17516161. DOI: [10.1016/j.jmbbm.2011.12.003](https://doi.org/10.1016/j.jmbbm.2011.12.003). URL: <http://dx.doi.org/10.1016/j.jmbbm.2011.12.003>.
- [33] T. J. Sill and H. A. von Recum. "Electrospinning: Applications in drug delivery and tissue engineering." In: *Biomaterials* 29.13 (2008), pp. 1989–2006. ISSN: 01429612. DOI: [10.1016/j.biomaterials.2008.01.011](https://doi.org/10.1016/j.biomaterials.2008.01.011).
- [34] M. Skotak, J. Ragusa, D. Gonzalez, and A. Subramanian. "Improved cellular infiltration into nanofibrous electrospun cross-linked gelatin scaffolds templated with micrometer-sized polyethylene glycol fibers." In: *Biomedical Materials* 6.5 (2011), pp. 1–20. ISSN: 1748605X. DOI: [10.1088/1748-6041/6/5/055012](https://doi.org/10.1088/1748-6041/6/5/055012). arXiv: [NIHMS150003](https://arxiv.org/abs/NIHMS150003).
- [35] N. Thadavirul, P. Pavasant, and P. Supaphol. "Development of polycaprolactone porous scaffolds by combining solvent casting, particulate leaching, and polymer leaching techniques for bone tissue engineering." In: *Journal of Biomedical Materials Research - Part A* 102.10 (2014), pp. 3379–3392. ISSN: 15524965. DOI: [10.1002/jbm.a.35010](https://doi.org/10.1002/jbm.a.35010).
- [36] Y. Wang, B. Wang, G. Wang, T. Yin, and Q. Yu. "A novel method for preparing electrospun fibers with nano-/micro-scale porous structures." In: *Polymer Bulletin* 63.2 (2009), pp. 259–265. ISSN: 01700839. DOI: [10.1007/s00289-009-0078-3](https://doi.org/10.1007/s00289-009-0078-3).
- [37] J. Wu and Y. Hong. "Enhancing cell infiltration of electrospun fibrous scaffolds in tissue regeneration." In: *Bioactive Materials* 1.1 (2016), pp. 56–64. ISSN: 2452199X. DOI: [10.1016/j.bioactmat.2016.07.001](https://doi.org/10.1016/j.bioactmat.2016.07.001). URL: <http://linkinghub.elsevier.com/retrieve/pii/S2452199X16300135>.
- [38] R. Yao, J. He, G. Meng, B. Jiang, and F. Wu. "Electrospun PCL/Gelatin composite fibrous scaffolds: Mechanical properties and cellular responses." In: *Journal of Biomaterials Science, Polymer Edition* 27.9 (2016), pp. 824–838. ISSN: 15685624. DOI: [10.1080/09205063.2016.1160560](https://doi.org/10.1080/09205063.2016.1160560).

-
- [39] J. J. Yoon, J. H. Kim, and T. G. Park. "Dexamethasone-releasing biodegradable polymer scaffolds fabricated by a gas-foaming/salt-leaching method." In: *Biomaterials* 24.13 (2003), pp. 2323–2329. ISSN: 01429612. DOI: [10.1016/S0142-9612\(03\)00024-3](https://doi.org/10.1016/S0142-9612(03)00024-3).
- [40] H. Yoshimoto, Y. M. Shin, H. Terai, and J. P. Vacanti. "A biodegradable nanofiber scaffold by electrospinning and its potential for bone tissue engineering." In: *Biomaterials* 24.12 (2003), pp. 2077–2082. ISSN: 01429612. DOI: [10.1016/S0142-9612\(02\)00635-X](https://doi.org/10.1016/S0142-9612(02)00635-X).
- [41] N. E. Zander, J. A. Orlicki, A. M. Rawlett, and T. P. Beebe. "Electrospun polycaprolactone scaffolds with tailored porosity using two approaches for enhanced cellular infiltration." In: *Journal of Materials Science: Materials in Medicine* 24.1 (2013), pp. 179–187. ISSN: 09574530. DOI: [10.1007/s10856-012-4771-7](https://doi.org/10.1007/s10856-012-4771-7).
- [42] Y ZHANG, S RAMAKRISHNA, C LIM, T PHAN, E CHONG, I LIM, and B BAY. "Evaluation of electrospun PCL/gelatin nanofibrous scaffold for wound healing and layered dermal reconstitution." In: *Acta Biomaterialia* 3.3 (2007), pp. 321–330. ISSN: 17427061. DOI: [10.1016/j.actbio.2007.01.002](https://doi.org/10.1016/j.actbio.2007.01.002).
- [43] J. Zhong, J. B. Baquiran, N. Bonakdar, J. Lees, Y. W. Ching, E. Pugacheva, B. Fabry, and G. M. O'Neill. "NEDD9 stabilizes focal adhesions, increases binding to the extra-cellular matrix and differentially effects 2D versus 3D cell migration." In: *PLoS ONE* 7.4 (2012). ISSN: 19326203. DOI: [10.1371/journal.pone.0035058](https://doi.org/10.1371/journal.pone.0035058).
- [44] S. Zhong, Y. Zhang, and C. T. Lim. "Fabrication of Large Pores in Electrospun Nanofibrous Scaffolds for Cellular Infiltration: A Review." In: *Tissue Engineering Part B: Reviews* 18.2 (2012), pp. 77–87. ISSN: 1937-3368. DOI: [10.1089/ten.teb.2011.0390](https://doi.org/10.1089/ten.teb.2011.0390). URL: <http://online.liebertpub.com/doi/abs/10.1089/ten.teb.2011.0390>.

